



INSTITUT NATIONAL DE RECHERCHE EN INFORMATIQUE ET EN AUTOMATIQUE

*Mathematical study of a neural gain control
mechanism*

Adrien Wohrer

N° 6327

October 2007

Thème BIO

*Rapport
de recherche*



Mathematical study of a neural gain control mechanism

Adrien Wohrer*

Thème BIO — Systèmes biologiques
Projet Odyssee

Rapport de recherche n° 6327 — October 2007 — 47 pages

Abstract: This report presents a dynamical mechanism of gain control, inspired by a simple membranar model for neurons. Mathematical results are enounced for the system under sinusoidal stimulation. We thus prove that the system induces under-linearity with input ampitude, and time advance for high input amplitudes, which are the dual mark of *contrast gain control* in retinal neurons.

Key-words: Gain control, neuron, feedback, shunting inhibition, retina

* Adrien.Wohrer@sophia.inria.fr

Étude mathématique d'un contrôle de gain neuronal

Résumé : Ce rapport présente un mécanisme dynamique de contrôle de gain, inspiré par un modèle de membrane de neurone. Des résultats mathématiques sont obtenus dans le cas d'une stimulation sinusoïdale du système. Nous prouvons ainsi que le système est sous-linéaire vis-à-vis de l'amplitude en entrée, et qu'il subit une avance de phase aux fortes amplitudes; ces deux propriétés sont la marque du *contrôle de gain au contraste* dans les cellules rétinienne.

Mots-clés : Contrôle de gain, neurone, feedback, *shunting inhibition*, rétine

Contents

1	Introduction	4
1.1	The underlying low-pass linear system	5
1.1.1	Characterizing the linear response to sinusoidal stimulation	5
1.2	Gain control through the nonlinear system	6
1.2.1	Characterizing the nonlinear response to sinusoidal stimulation	6
1.2.2	Reducing the system's dimensionality	7
2	General study of the gain control system	7
2.1	System definition and first properties	7
2.1.1	System definition	7
2.1.2	Notations	8
2.1.3	Periodic asymptotic solution of the system	10
2.2	Numerical simulation	14
2.2.1	General behavior of the system	14
2.2.2	Gain control on input amplitude	16
2.2.3	Parameter b defines the shape of the phase portrait	18
3	Asymptotic behavior $b = 0$	20
3.1	System definition	20
3.2	Dependence of V_{\max} and ϕ_{\max} w.r.t. system parameters	21
4	Asymptotic behavior $b = +\infty$	23
4.1	System definition	23
4.2	Integral formulations for partial derivatives in the system	26
4.3	Dependence of V_{\max} and ϕ_{\max} w.r.t. system parameters	30
4.3.1	Dependence w.r.t. A (Points (iii)-(vi)).	31
4.3.2	Dependence w.r.t. ω (Points (i)-(ii))	35
4.4	Local under-linearity of V_{\max} w.r.t. A	37
5	A track for the future: Perturbation analysis	39
5.1	Perturbation analysis near $b \rightarrow +\infty$	40
5.2	Perturbation analysis near $b \rightarrow 0$	43
	Conclusion	46

1 Introduction

We have proposed in previous work the use of a particular dynamical system, based on feedback, to provide *contrast gain control* in a model of retinal processing [3, 2]. The equations of this system were the following:

$$\frac{dV}{dt}(x, y, t) = I(x, y, t) - G(x, y, t)V(x, y, t) \quad (1)$$

$$G(x, y, t) = G_\sigma \overset{x,y}{*} E_\tau \overset{t}{*} Q(V)(x, y, t), \quad (2)$$

$$Q(v) = Q_0 + \lambda v^2, \quad (3)$$

where $V(x, y, t)$ is a spatial map representing the membrane potentials of the cells where the gain control is taking place, and $G(x, y, t)$ is a variable conductance term driven by the recent values of $V(x, y, t)$. $G(x, y, t)$ is obtained from $V(x, y, t)$ through two successive steps. First, the point-by-point application of a function Q which is taken *positive, convex and symmetrical*. Second, the application of a *linear, spatio-temporal averaging*, through temporal convolution by the Exponential kernel

$$E_\tau(t) = \tau^{-1} \exp(-t/\tau) \mathbf{1}_{t>0},$$

and spatial convolution by the Gaussian kernel

$$G_\sigma(x, y) = \exp(-(x^2 + y^2)/(2\sigma^2))/(2\pi\sigma^2)$$

(which is bound to disappear soon from our equations, as we will make our system purely temporal).

System (1)-(3) has been heuristically found efficient in reproducing the change of shape in temporal kernels typical of contrast gain control in the retina [3, 2]. However, because it is nonlinear, the exact response of such a system is not trivial, and a rigorous mathematical analysis appears difficult in the general case. Missing this mathematical analysis is problematic. Indeed, if the system is bound to be implemented in a bio-inspired model, one would like guarantees that it does not induce spurious effects (resonances, etc.) for certain sets of system parameters or input signals.

In fact, the gain control loop (1)-(3) appears to be very stable experimentally. Heuristically, the system is stable because it is a simple extension of a linear ‘RC’ circuit (a stable system if ever), only with a resistance R which varies dynamically. In this report, we try to provide a more rigorous explanation of the system’s stability, through a mathematical analysis of the system’s response to a simple type of input: Sinusoidal stimulation.

Here is the plan of this report. Our gain control loop is the nonlinear extension of an ‘RC’ circuit. We thus start by studying this low-pass, linear filter, as a benchmark for comparison with our nonlinear system (Section 1). A necessary reduction of dimensionality leads us to the object of our study in this chapter, a 2-dimensional nonlinear control loop. We study its behavior through general properties and numerical simulation (Section 2).

Unfortunately, precise mathematical proofs are still out of reach in the general case of this 2D system. However, studying the phase portraits of the system for different sets of parameters reveals the existence of two asymptotic behaviors, at both extrema of one particular parameter's definition domain, for which the dimensionality of the system is reduced to 1D. In Sections 3 and 4, we derive precise mathematical results for the two respective 1D asymptotic systems.

Finally, in Section 5, we give first hints of how perturbation analysis may allow to increase the range of parameters in which the system is mathematically tractable.

1.1 The underlying low-pass linear system

We start by making explicit the links of the gain control loop (1)-(3) with a simple 'RC' circuit. This analysis will help us to define a characterization of 'good behavior' for our nonlinear system.

The gain control loop (1)-(3) has been designed as an extension of a temporal *low-pass* system. Indeed, when the strength of the feedback in (3) is taken as $\lambda = 0$, (2) becomes the trivial relation $G(x, y, t) = Q_0$ (because filters $G_\sigma(x, y)$ and $E_\tau(t)$ both have a gain of 1), and in turn (1) writes:

$$\frac{dV}{dt}(x, y, t) = I(x, y, t) - Q_0 V(x, y, t), \quad (4)$$

which is a simple 'RC' low-pass temporal filter. Because system (4) is linear, it is completely described by its Fourier transform:

$$\tilde{H}(\omega) = 1/(Q_0 + \mathbf{j}\omega). \quad (5)$$

1.1.1 Characterizing the linear response to sinusoidal stimulation

A linear system is totally characterized by its response to a sinusoidal input:

$$\frac{dV}{dt}(t) = A \cos(\omega t) - Q_0 V(t). \quad (6)$$

When a solution $V(t)$ follows (6), its initial response depends on its initial conditions. But the initial conditions are forgotten asymptotically fast, and all solutions finally converge to a single trajectory which is also sinusoidal at pulsation ω , and hence fully described by two numbers:

1. Its maximum value V_{\max} , corresponding to the amplitude of $V(t)$, given by

$$V_{\max} = |\tilde{H}(\omega)|A. \quad (7)$$

2. The time t_{\max} when V_{\max} is reached (in each sinus cycle), which provides the phase difference of $V(t)$ with its input current:

$$\phi_{\max} = \omega t_{\max} = \arg(\tilde{H}(\omega)) \pmod{2\pi}. \quad (8)$$

Both formulas (7) and (8) rely on the Fourier transform (5).

Interestingly, V_{\max} and t_{\max} provide a good characterization of the dependence of system (6) w.r.t. parameters A and ω of the input current:

Dependence w.r.t. input frequency ω . The dependence of V_{\max} and t_{\max} w.r.t ω is typical of a *low-pass* system:

$$\partial_{\omega} V_{\max} < 0, \text{ and } \lim_{\omega \rightarrow +\infty} V_{\max} = 0, \quad (9)$$

$$\partial_{\omega} \phi_{\max} > 0, \text{ and } \lim_{\omega \rightarrow +\infty} \phi_{\max} = \pi/2 \pmod{2\pi}. \quad (10)$$

In words, (9) states that the response magnitude decreases with frequency towards 0 for large values, while (10) states that the phase delay of the response increases with frequency, towards phase quadrature.

Dependence w.r.t. input amplitude A . The dependence of V_{\max} and ϕ_{\max} w.r.t. A is trivial, since the system is linear:

$$\partial_A V_{\max} = |\tilde{H}(\omega)| > 0, \text{ and } \partial_A (V_{\max}/A) = 0 \quad (11)$$

$$\partial_A \phi_{\max} = 0 \quad (12)$$

In words, (11) states that the magnitude of response is simply proportional to the input amplitude, and (12) states that the phase (and thus, time of peak) of the response is independent of amplitude.

1.2 Gain control through the nonlinear system

1.2.1 Characterizing the nonlinear response to sinusoidal stimulation

In this chapter, we wish to study mathematically the *nonlinear* case, when feedback (2)-(3) has an effective strength $\lambda > 0$. For such a nonlinear system, Fourier analysis cannot be used simply anymore, so we cannot hope to fully characterize the system's response to *any* type of stimulus based only on the response to a sinus.

However, sinusoidal stimulation still has some descriptive power: It allows to test the system's response to stimuli of different amplitudes A , and different 'speeds of variation', as measured by the sinus' frequency ω . For this reason, our study of the nonlinear system also focuses on input currents of the form $I(t) = A \cos(\omega t)$, and still uses V_{\max} and ϕ_{\max} as good indicators of the system's behavior.

More precisely, our ultimate goal is to find equivalents to formulas (9)-(12) in the nonlinear case, proving the good behavior of our system. Concerning the behavior w.r.t. to input frequency ω , we want to prove that formulas (9)-(10) still hold, meaning that our system is still 'low-pass', as measured by the amplitude V_{\max} of its response.

By opposition, concerning the behavior w.r.t. input amplitude A , we would like to prove a different behavior than (11)-(12) for our nonlinear system. Indeed, the system intends to be a *gain control* mechanism. Instead of (11), we would thus like to show that

$$\partial_A V_{\max} > 0, \text{ and } \partial_A (V_{\max}/A) < 0. \quad (13)$$

The first relation means that the system still responds with increasing amplitude to increasing contrasts (an important behavior to be verified!). However, the growth with A should be now *under-linear* (second relation), thus proving the presence of gain control.

Also, we would like to prove the phase advance at high amplitudes, which is a typical expression of contrast gain control in the retina [3, 2]. Instead of (12), we would thus like to show that

$$\partial_A \phi_{\max} < 0.$$

1.2.2 Reducing the system's dimensionality

In general, nonlinear systems get exponentially hard to study as the dimension of the space they live in increases. Systems of dimensions 1 and 2 are fairly understood, but chaotic behaviors and increased mathematical difficulty appear from dimension 3 on.

Unfortunately, the dimensionality of the original system (1)-(3) is particularly high, making mathematical analysis very difficult. As a consequence, we will proceed to successive simplifications of our system.

1. The spatial structure (x, y) of the equations, which is coupled with time by (2), provides an infinite dimensionality to system (1)-(3). To derive mathematical results, we must ignore this spatial structure, and study only the temporal evolution of two coupled variables $V(t)$ and $G(t)$, driven by an input current $I(t)$.
2. After the preceding simplification, we are left with a dynamic system (V, G) of dimension 2, but which is not *autonomous*, because the input current $I(t)$ varies in time. The equivalent autonomous system (by adding I , or t , to the system) is of dimension 3, and this is already a difficult dimensionality. We will see in the sequel how in particular limit cases, system (1)-(3) can further be simplified to a 1- (2- if autonomous) dimensional system.

For the moment, let us start by introducing our general 2D system (V, G) and its first properties.

2 General study of the gain control system

2.1 System definition and first properties

2.1.1 System definition

The system under study is that of a cell or population of cells with membrane potential $V(t)$, that integrates an input current $I(t) = A \cos(\omega t)$ under dynamic gain control from conductances $G(t)$ in its membrane. $(V(t), G(t))$ is driven by

$$\begin{cases} \dot{V}(t) = A \cos(\omega t) - G(t)V(t), & (a) \\ \dot{G}(t) = b(Q(V(t)) - G(t)), & (b) \end{cases} \quad (14)$$

where the dot denotes temporal derivation, b is a strictly positive parameter, and $Q(v)$ is a strictly positive, even and convex¹ function with sufficient regularity (see Figure 1). We note $Q_0 = Q(0) > 0$.

Leak function Q . We refer to $v \rightarrow Q(v)$ as the *leak function* of the system, because it defines the leaks $G(t)$ in the cellular membranes modeled by (14-a). More precisely, Q can always be decomposed as

$$Q(v) = \tilde{Q}(v) + Q_0,$$

with $\tilde{Q}(0) = 0$ and $Q_0 > 0$. Since equation (14-b) is linear with a gain of 1, this decomposition of Q translates to a decomposition of $G(t)$: $G(t) = \tilde{G}(t) + Q_0$, where $\tilde{G}(t)$ is the part of $G(t)$ linearly driven by $\tilde{Q}(V(t))$. Note that

$$G(t) \geq Q_0 > 0,$$

because $G(t)$ is a low-passed version of $Q(V(t))$. Note that mathematically, we must also *impose* this ‘physical’ property of $G(t)$ on our initial condition: $G(0) \geq Q_0$.

In turn, the leak current in (14-a) can be written

$$-G(t)V(t) = -\tilde{G}(t)V(t) - Q_0V(t),$$

so that Q_0 corresponds to the *static leaks* in the cellular membrane, and $\tilde{G}(t)$ to the ‘purely dynamic’ leaks.

Cut-off frequency for the adaptation b . As compared to (1)-(3), we have noted $b = \tau^{-1}$. Parameter b , expressed in Hertz, measures the rapidity with which $G(t)$ ‘sticks’ to its driving input $Q(V(t))$. This parameter will have a strong influence on the qualitative behavior of the system (Section 2.2.3).

2.1.2 Notations

Various differentiations in the system. Throughout this chapter, we will encounter different types of differentiations and derivatives. Here are the general notations we will be using:

- Notation $\dot{f}(t)$ (or directly $\frac{df}{dt}$) represents the derivative w.r.t. time of function $f(t)$.
- Notation $F'(v)$ represents the derivative w.r.t. v of function $F(v)$, where v has the dimension of our variable $V(t)$ (originally, a membrane potential).
- Notation $\partial_p X$ represents the partial derivative of X (any scalar or vector) w.r.t. a parameter p of the system (typically, $p = A$).

¹For many results in this chapter, it is sufficient to consider Q strictly positive, even, and such that $\forall v, vQ'(v) \geq 0$. However, the supplementary requirement that Q be convex appears in some results. For simplicity, we prefer to assume it from the start.

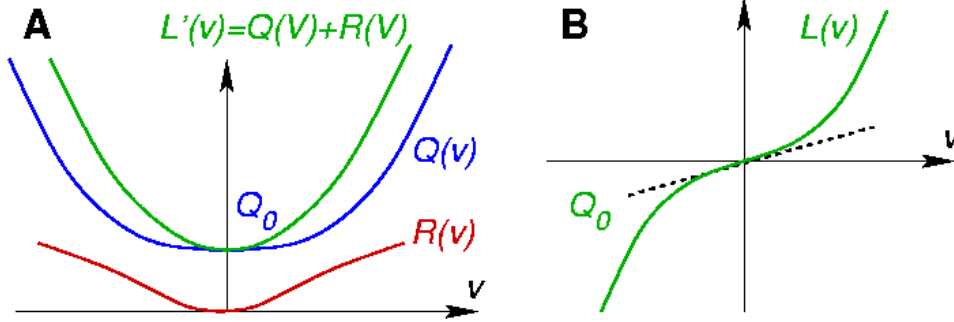


Figure 1: Schematic representations of functions $Q(v)$, $R(v) = vQ'(v)$ (panel A), $L(v) = vQ(v)$ (panel B), and $L'(v) = Q(v) + R(v)$ (panel A).

- *Gâteaux derivatives.* Let a scalar/vector X depend on a particular function F (amongst other parameters):

$$X(F, \dots),$$

and let F_2 be a function of the same nature as F . If it exists, we will note $\partial_F^{(F_2)} X$ the *Gâteaux derivative* of X when F is modified along F_2 :

$$\partial_F^{(F_2)} X = \lim_{\varepsilon \rightarrow 0} \frac{X(F + \varepsilon F_2, \dots) - X(F, \dots)}{\varepsilon}.$$

Note that, for two well-defined Gâteaux derivatives $\partial_F^{(F_1)} X$ and $\partial_F^{(F_2)} X$, one has $\partial_F^{(F_1 + F_2)} X = \partial_F^{(F_1)} X + \partial_F^{(F_2)} X$.

- *Function derivatives.* If $X : t \in \mathbb{R} \rightarrow X(t)$ is a function of time, then $\partial_p X(t)$ represents the partial derivative along p of $X(t)$, t being held constant.

Remark: In all cases considered here, the function $t \rightarrow \partial_p X(t)$ so defined also corresponds to the partial derivative of *function* $t \rightarrow X(t)$ w.r.t. p for norm $\| \cdot \|_\infty$ over \mathbb{R} . This is because all partial derivatives considered will be T -periodic by construction, as stated in Point (iii) of Proposition 1. ■

Functions derived from $Q(v)$. Due to the intrinsic nature of system (14), we will repeatedly come across a number of algebraical expressions derived from function $v \rightarrow Q(v)$. For the sake of concision, we find it convenient to name these secondary functions.

We will first consider function

$$R(v) = vQ'(v) \geq 0, \quad (15)$$

which is always positive because $Q(v)$ is convex and even.

We will also consider the diffeomorphism from \mathbb{R} to itself:

$$L(v) = vQ(v), \quad (16)$$

which is indeed bijective since

$$L'(v) = Q(v) + R(v) \geq Q(v) \geq Q_0 > 0. \quad (17)$$

Functions $Q(v)$, $R(v)$, $L(v)$ and $L'(v)$ are schematically represented in Figure 1.

2.1.3 Periodic asymptotic solution of the system

We have seen in Section 1.1.1 that in the ‘linearized’ version of our system, $V(t)$ tends asymptotically fast to a sinusoidal response, possibly after some initial transient due to its initial conditions. The following proposition generalizes this behavior to nonlinear system (14).

Proposition 1 *Let A , ω and $b \in \mathbb{R}^{+*}$. Let $v \rightarrow Q(v)$ be an even, convex, strictly positive function with sufficient regularity, and $Q(0) = Q_0 > 0$. Let $T = 2\pi/\omega$.*

(i) *The following equation on $Z(t) = (X(t), Y(t))$:*

$$\dot{Z}(t) = \begin{pmatrix} \dot{X}(t) \\ \dot{Y}(t) \end{pmatrix} = \begin{pmatrix} A \cos(\omega t) - X(t)Y(t) \\ b(Q(X(t)) - Y(t)) \end{pmatrix} \quad (18)$$

admits a unique T -periodic solution that we note $W(t) = (V(t), G(t))$. All other solutions $Z(t)$ with initial condition $Y(0) \geq Q_0$ converge exponentially fast to $W(t)$.

(ii) *$V(t)$ is $T/2$ -antiperiodic, and $G(t)$ is $T/2$ -periodic:*

$$\begin{aligned} V(t) &= -V(t + T/2) \\ G(t) &= G(t + T/2). \end{aligned}$$

(iii) *Function $W : t \rightarrow W(t)$ admits C^1 differentiation w. r. t. parameters A and b and Gâteaux derivatives w.r.t. function Q , in the space of ($T/2$ -antiperiodic, $T/2$ -periodic) functions with norm $\|\cdot\|_\infty$.*

Remark: Differentiation w.r.t. parameter ω .

Concerning Point (iii), remark that parameter ω has not been included in the parameters with respect to which differentiation is possible. Indeed, even a small change of frequency $\omega \rightarrow \omega + \varepsilon$ leads to a strong divergence between the asymptotic trajectories $W_\omega(t)$ and $W_{\omega+\varepsilon}(t)$, since they have different periods!

However, the scalar quantities V_{\max} and ϕ_{\max} (defined on the asymptotic periodic solution $V(t)$) are differentiable w.r.t. ω . To study their dependence, a good solution is to introduce the change of parametrization $\phi = \omega t$, $\tilde{Y} = Y/\omega$, through which (18) becomes

$$\frac{d}{d\phi} \tilde{Z}(\phi) = \begin{pmatrix} \frac{d}{d\phi} X(\phi) \\ \frac{d}{d\phi} \tilde{Y}(\phi) \end{pmatrix} = \begin{pmatrix} \frac{A}{\omega} \cos(\phi) - X(\phi)\tilde{Y}(\phi) \\ b(\frac{1}{\omega}Q(X(t)) - \tilde{Y}(t)) \end{pmatrix}$$

In this new system, differentiation w.r.t. ω is possible (see the sequel). ■

The proof of Proposition 1 relies on the fact that system (18) is *contracting*, as defined in [1]. In the following paragraph, we remind the main properties of a contracting system. In a second paragraph, we present a general proposition on periodic contracting systems, which will apply to the system considered here. In a third paragraph, we show that system (18) is indeed contracting, and thus prove Proposition 1.

Contracting system

A dynamic system $\dot{Z}(t) = F(Z(t), t)$ defined in an open set Ω of a Banach E , is said to be *contracting* if $F(Z, t)$ admits a differential $dF(Z, t)$ w.r.t. its first variable, and a strictly negative upper bound $-\lambda_0 < 0$ can be found for the real parts of the eigenvalues of $dF(Z, t)$, independently of $t \in \mathbb{R}$ and $Z \in \Omega$ [1]. Or equivalently:

$$\forall t \in \mathbb{R}, \forall Z \in \Omega, \forall X \in E, \quad X^T dF(Z, t) X \leq -\lambda_0 \|X\|^2. \quad (19)$$

Such a system is characterized by an exponential convergence of all its solutions to a unique trajectory, independently of their initial condition [1]. Contraction is thus the warrant of a strong *stability* for the system.

We remind the main result when a system is contracting. If we consider two solutions $Z_1(t)$ and $Z_2(t)$, starting at time $t = 0$ with different initial conditions, then

$$\frac{d}{dt} (\|Z_1 - Z_2\|^2) = 2(Z_1 - Z_2)(F(Z_1, t) - F(Z_2, t)) \leq -\lambda_0 \|Z_1 - Z_2\|^2,$$

where the last inequality is a consequence of (19), when $dF(Z, t)$ is integrated between $Z_1(t)$ and $Z_2(t)$ along $Z_2(t) - Z_1(t)$. From Gronwall's Lemma, the last inequality can be integrated, yielding

$$\|Z_1(t) - Z_2(t)\|^2 \leq \|Z_1(0) - Z_2(0)\|^2 \exp(-\lambda_0 t). \quad (20)$$

So, after some initial transient that depends on their initial condition, all solutions $Z(t)$ converge to a 'unique' asymptotic trajectory.

Unique periodic solution of a contracting system

To prove Proposition 1, we must use the contracting properties of system (18), in the particular case of a periodic input $A \cos(\omega t)$. The following general proposition describes the asymptotic behavior of a periodic contracting system: The system's asymptotic response is also periodic, and depends continuously on the parameters of the system.

Proposition 2 (Periodic contracting system) Consider a T -periodic contracting dynamic system defined on an open set $Z \in \Omega$:

$$\frac{d}{dt} Z = F(Z(t), t, p), \quad (21)$$

where:

- p is any parameter of the system such that F has a C^1 dependence on p .
- Function F is T -periodic for a certain $T > 0$, in the sense that

$$\forall t, \forall p, \forall Z \in \Omega, \quad F(Z, t + T, p) = F(Z, t, p).$$

- Contraction property: F is C^1 w.r.t. Z , and its differential $dF(Z, t, p)$ admits a strictly negative upper bound $-\lambda_0 < 0$ on the real part of its eigenvalues, independently of t and $Z \in \Omega$ (possibly, λ_0 can depend on p).

Then, the asymptotic behavior of the system is characterized by the two following points:

- For any value of parameter p , system (21) admits a unique T -periodic solution that we note $W(t, p)$ (or simply $W(t)$). Since the system is contracting, all other solutions of (21) converge exponentially fast to $W(t)$.
- Structural stability of the asymptotic solution: Function $W : (t, p) \rightarrow W(t, p)$ is C^1 .

Heuristically, Point (i) of this proposition states that any solution $Z(t)$ of a T -periodic contracting system rapidly becomes T -periodic itself, once that its initial conditions are forgotten and it is entirely driven by the nature of its input. Naturally, amongst the bundle of all solutions $Z(t)$ which are ‘asymptotically periodic’ (and converging to a ‘unique’ trajectory), there must exist a ‘central’ solution $W(t)$ that is *exactly* T -periodic.

As for Point (ii) of this proposition, it is strongly reminiscent of the local C^1 dependence of the solutions of an ODE w.r.t. to system parameters, as stated by the Cauchy-Lipschitz Theorem on the existence of local solutions to an ODE. The whole point here is to extend the *local* C^1 dependence, for any solution $Z(t)$, to a *global* C^1 dependence for the asymptotic trajectory, as ‘materialized’ by the unique periodic solution $W(t)$.

Proof of Proposition 2

An easy proof of Proposition 2 can be given, relying on the parametric version of Picard’s *fixed point theorem*. Consider $\phi_T : \Omega \rightarrow \Omega$ the application sending each point to its ‘image at time T ’ following ODE (21):

$$\forall Z \in \Omega, \quad \phi_T(Z) = \Phi(T, 0, Z, p),$$

where $\Phi(t, t_0, Z_0, p)$ is the *flow* associated to (21), i.e., the unique solution of (21) at time t with initial condition Z_0 at time t_0 .

The fact that system (21) is ‘contracting’, in the sense of (20), implies that *function* ϕ_T is ‘contracting’, in the sense needed by Picard’s theorem:

$$\forall Z_1, Z_2 \in \Omega, \quad \|\phi_T(Z_1) - \phi_T(Z_2)\| \leq \|Z_1 - Z_2\| \exp(-\lambda_0 T/2).$$

As a result, Picard’s theorem insures that function ϕ_T admits a unique *fixed point* $W_0(p)$ in Ω , such that

$$W_0(p) = \Phi(T, 0, W_0(p), p). \tag{22}$$

Let us then note $W(t, p) = \Phi(t, 0, W_0(p), p)$. It is by definition a solution of ODE (21). Because of (22) and the fact that function F is periodic, $W(t, p)$ is T -periodic. Also, since (22) characterizes a unique possible point $W_0(p) = W(0, p)$, the whole solution $W(t, p)$ is unique.

Finally, Picard's theorem exists in a *parametric* form: If the contracting function considered (here, function ϕ_T) has a C^1 dependance on some parameter p , so does its unique fixed point. This insures the C^1 dependance of $W_0(p)$ w.r.t. system parameters p . But the flow $\Phi(t, t_0, Z_0, p)$ is also C^1 w.r.t. its four arguments, from the Cauchy-Lipschitz (aka Picard-Lindelöf) theorem. By composition, $W(t, p) = \Phi(t, 0, W_0(p), p)$ is thus C^1 w.r.t. p . \square

Proof of Proposition 1

Let us prove the contracting properties of system (18). In our case, $\Omega = \{Z = (X, Y) | Y \geq Q_0\}$ (by hypothesis for the initial condition $Y(0)$, and then because $Q(X(t)) \geq Q_0$). The system can be rewritten

$$\dot{Z}(t) = \begin{pmatrix} A \cos(\omega t) \\ 0 \end{pmatrix} - J(Z(t)), \quad (23)$$

with

$$J(Z) = \begin{pmatrix} XY \\ b(Y - Q(X)) \end{pmatrix}, \quad (24)$$

and the differential of J w.r.t. Z verifies the following property:

$$\det(dJ(Z) - \lambda \text{Id}) = \lambda^2 - (Y + b)\lambda + b[Y + R(X)],$$

with $R(v) = vQ'(v) \geq 0$ (from (15)). Then, if we denote λ_1 and λ_2 the two eigenvalues of $dJ(Z)$, straightforward calculus proves that:

$$\forall Z \in \Omega, \quad \max(\mathcal{R}(\lambda_1), \mathcal{R}(\lambda_2)) \geq \min(Q_0, b) \triangleq \lambda_0 > 0, \quad (25)$$

so that λ_0 , defined by (25), is a strictly positive lower bound for the real parts of the eigenvalues of $dJ(Z(t))$, independently of t and the solution $Z(t)$ considered. This proves that the system is contracting, following the definition given above.

Because system (18) is contracting and periodic, Proposition 2 directly provides Points (i) and (iii) of Proposition 1.

To prove Point (ii), note that the input sinus itself is $T/2$ -antiperiodic: $A \cos(\omega(t + T/2)) = -A \cos(\omega t)$, so that $(-V(t + T/2), G(t + T/2))$ is also a T -periodic solution of (18). By unicity of the periodic solution, $W(t) = (-V(t + T/2), G(t + T/2))$. \square

Remark: Note that Point (iii) of Proposition 1 also implies that the system ODE (18) can be differentiated w.r.t. any system parameter p , yielding a new ODE which drives $\partial_p W(t)$. We will often apply this technique in the sequel. \blacksquare

2.2 Numerical simulation

When it comes to quantitative analysis, such as characterizing the maximum V_{\max} of $V(t)$ over a cycle (the ultimate goal of the chapter, see Section 1.2), system (14) is particularly hard to study: Its complexity is equivalent to that of a 3-dimensional autonomous system (Section 1.2). As a result, we could not provide any quantitative mathematical results for the general case of system (14).

Instead, we simulated (14) for different sets of parameters, to gain a ‘heuristic’ understanding of the system. We thus found that, whatever set of parameters used, the under-linear dependence (13) of V_{\max} w.r.t. input amplitude A appears to hold. We also found that the shape of the phase portrait of $W(t) = (V(t), G(t))$ is strongly influenced by the value of the cut-off parameter b for the adaptation conductance. We now present these results.

2.2.1 General behavior of the system

Because system (14) is contracting, it reaches its asymptotic periodic trajectory $W(t)$ exponentially fast, with a typical time constant λ_0^{-1} , with $\lambda_0 = \min(b, Q_0)$. When the phase portrait of $W(t) = (V(t), G(t))$ is plotted, it displays a symmetric shape, because of the system’s typical symmetry (Proposition 1, Point (ii)). The resulting curve, displayed² in Figure 2, can evoke different objects according to the viewer’s frame of mind. In the scope of this thesis, we refer to it as a ‘butterfly’ curve. . .

Along with the evolution of $W(t)$, Figure 2 represents the evolution of some other ‘relevant’ 2D points (see legend).

For example, at each time t_0 , we define point $W_\infty(t_0) = (V_\infty(t_0), G_\infty(t_0))$ as the (unique) equilibrium point if the system was let to evolve for $t > t_0$ with an input current held constant at $I(t) = A \cos(\omega t_0)$ (Since the system is contracting, all other solutions would also converge exponentially fast to $W_\infty(t_0)$). This ‘instantaneous’ equilibrium point is computed by solving ($\dot{V} = 0, \dot{G} = 0$), which has a unique solution:

$$\begin{cases} V_\infty(t)Q(V_\infty(t)) = A \cos(\omega t) \\ G_\infty(t) = Q(V_\infty(t)) \end{cases} \quad (26)$$

Graphically, $(V_\infty(t), G_\infty(t))$ is obtained as the intersection of the convex, symmetric curve $G = Q(V)$ with the branch of hyperbola $GV = I(t) = A \cos(\omega t)$ (Figure 3).

In linear systems, the ‘instantaneous equilibrium point’ plays the role of a *driving force* on the system (see next remark). Although there is no such well-defined role for $W_\infty(t)$ in the nonlinear system presented here, $W_\infty(t)$ still appears to act pretty much like a driving force on $W(t)$, as can be seen in Figure 2 (see legend).

Remark: Driving potential in stable linear systems

When a stable linear dynamic $\dot{Z}(t) = \mathbf{A}(t)Z(t) + B(t)$ is considered (such that $\forall t$, the two eigenvalues of $\mathbf{A}(t)$

²The corresponding animated movie can be found at www-sop.inria.fr/odyssee/team/Adrien.Wohrer/retina/other_files/CGC_movie.mpg.

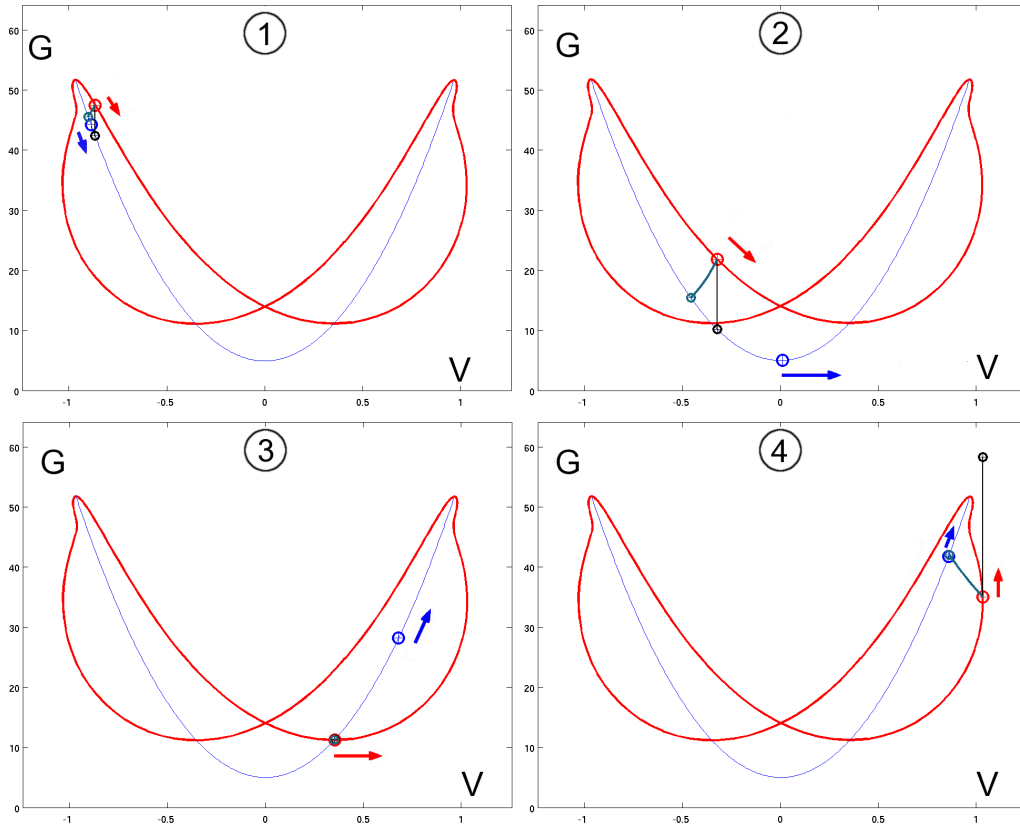


Figure 2: Evolution of system (14) over a half-period, for a typical set of parameters. The thick red curve is the phase portrait of $W(t) = (V(t), G(t))$: It typically revolves around the ‘driving curve’ defined by $G = Q(V)$ (thin blue curve). The current value of $W(t)$ is indicated by the large red dot, while the instantaneous equilibrium point $W_\infty(t)$ (see text) is indicated by the large blue dot. Although there is no trivial link between $W(t)$ and $W_\infty(t)$, the latter appears to ‘drive’ the former, since it is always ‘in advance’ in the phase portrait. Two other points are indicated in each figure: Point $(V(t), Q(V(t)))$ (small black dot) is coupled to the sign of $\dot{G}(t)$, whether it is over or under point $V(t)$ (vertical black line). See e.g. Panel 3 when $\dot{G}(t) = 0$. Point $(V_\pi(t), G_\pi(t))$ (small green dot) is the point on curve $G = Q(V)$ such that $V(t)G(t) = V_\pi(t)G_\pi(t)$. Its position relative to $W_\infty(t)$ is coupled to the sign of $\dot{V}(t)$. See e.g. Panel 4 when $\dot{V}(t) = 0$.

have strictly negative real parts), the instantaneous equilibrium point is defined by $\mathbf{A}(t)Z_\infty(t) + B(t) = 0$. The system's driving equation can thus be re-written $\dot{Z}(t) = \mathbf{A}(t)(Z(t) - Z_\infty(t))$.

As a result, function $Z(t)$ depends linearly on function $Z_\infty(t)$. In particular, there exists a kernel $\mathbf{K}(t, u)$ (with the dimension of a matrix), depending only on the nature of function $t \rightarrow \mathbf{A}(t)$ (generally without any analytic expression), such that $\forall t, Z(t) = \mathbf{K}(t, t)Z(0) + \int_{u=0}^t \mathbf{K}(t, u)Z_\infty(t-u)du$ and $\int_{u=0}^{+\infty} \mathbf{K}(t, u)du = 1$, meaning that once initial conditions are forgotten, $Z(t)$ is obtained as a linear *average* over the recent values of $Z_\infty(t)$. ■

2.2.2 Gain control on input amplitude

Now that we have described the typical behavior of $W(t)$, we can question more precisely the influence of the different parameters in the system. The dependence of $W(t)$ on amplitude A is particularly interesting to us, since we wish to prove the under-linearity of V_{\max} w.r.t. A (equation (13)).

And indeed, whatever set of parameters used in our simulations (b, ω and quadratic function $Q(v) = Q_0 + \lambda v^2$), we always found V_{\max} to be a growing function of A , and this growth to happen under-linearly.

A typical example of the system's dependence on input amplitude A is provided in Figure 4. Both $V(t)$ and phase portrait $(V(t), G(t))$ are represented, for different values of parameter A . The under-linearity w.r.t A can be observed, as well as the time advance of $V(t)$ as A increases (t_{\max} decreases with A). Note however that t_{\max} is not easily defined, as $V(t)$ can possibly display two maxima per cycle.

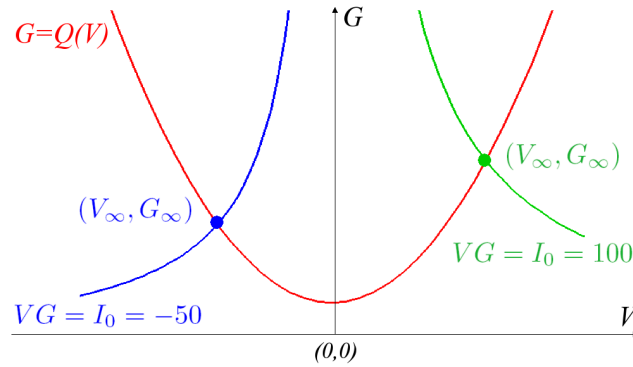


Figure 3: The instantaneous equilibrium point $W_\infty(t)$ of the system is graphically obtained at the intersection of curves $G = Q(V)$ and $GV = I(t) = A \cos(\omega t)$.

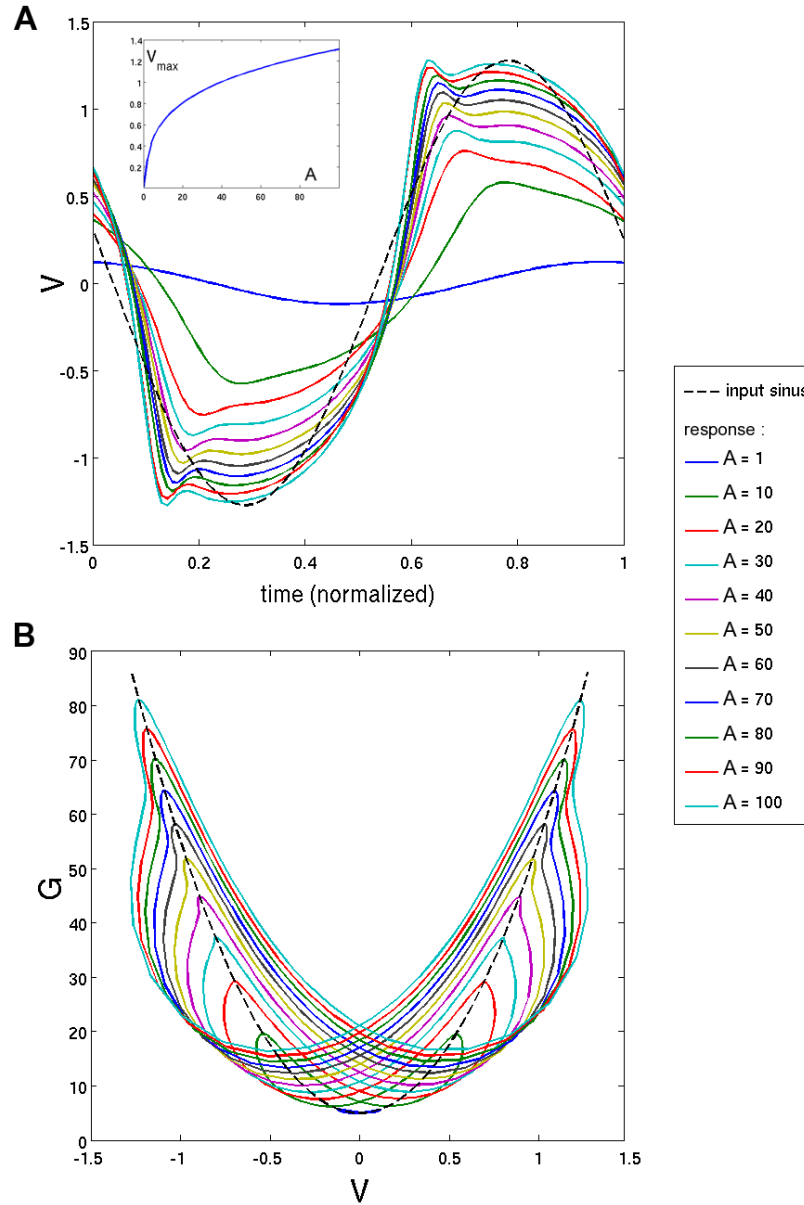


Figure 4: Response to an input sinusoidal current $I(t) = A \cos(\omega t)$ of increasing amplitude A . Panel A represents $V(t)$ over one period, and Panel B represents the phase portrait $(V(t), G(t))$. V_{\max} appears to be a growing function of A , but this growth is under-linear (inset curve plots V_{\max} against A). Also note the apparent phase advance for t_{\max} with increasing contrasts. At low input amplitudes (curve $A = 1$), the system behaves linearly, as the phase portrait remains in the zone ' $G \simeq Q_0$ '. Other simulation parameters: $\omega = 2\pi$ Hz, $b = 20$ Hz, $Q(V) = Q_0 + \lambda V^2$ with $Q_0 = 5$ Hz and $\lambda = 50$ Hz.

2.2.3 Parameter b defines the shape of the phase portrait

Parameter b defines the cut-off frequency for the integration of input $Q(V(t))$ by $G(t)$, through

$$\dot{G}(t) = b(Q(V(t)) - G(t)). \quad (27)$$

As a first remark, note that the value of b only has a ‘secondary’ effect on the typical *range of values* taken by $V(t)$ and $G(t)$. Indeed, the linear filter described by (27) has a gain of 1, so that $\widehat{G} = \widehat{Q(V)}$ independently of b , where the hat denotes averaging over one period of the system. As a result, the ‘typical’ orders of magnitude \widetilde{V} and \widetilde{G} of the system (a blurry notion if ever) can be defined by

$$\begin{cases} \widetilde{V}Q(\widetilde{V}) = A \\ \widetilde{G} = Q(\widetilde{V}), \end{cases}$$

independently of the value of parameter b .

A typical example of the system’s dependence on parameter b is provided in Figure 5, where both $V(t)$ and phase portrait $(V(t), G(t))$ are represented for different values of b , all other parameters being held constant. It can be seen that, even if parameter b does not have a strong influence on the typical range of values taken by the system, it has a strong influence on the general *shape* of the phase portrait.

In particular, two asymptotic behaviors for the system can be observed, when $b \rightarrow 0$ and when $b \rightarrow +\infty$ (more precisely, the determinant factor is bT , comparing b to the intrinsic frequency of the system). Both asymptotic behaviors are characterized by a reduction of dimensionality, as the limit systems appear to live in a 1-dimensional space only:

‘Flat’ limit when $b = 0$. When b gets close to 0, the filtering of $Q(V(t))$ to produce $G(t)$ becomes more and more low-pass, implying that $G(t)$ becomes close to a *constant* function. In Figure 5 B, this translates in a progressive flattening of the phase diagram. In Section 3, we propose a suitable characterization of the asymptotic limit ‘ $b = 0$ ’, in which $G(t) = G_0$ is imposed to be constant.

‘Convex’ limit when $b = +\infty$. When b gets close to $+\infty$, the filtering of $Q(V(t))$ to produce $G(t)$ becomes more and more high-pass, implying that $G(t)$ becomes close to $Q(V(t))$. In Figure 5 B, this translates in a phase diagram which ‘sticks’ to the driving curve $G = Q(V)$ (represented by a dotted line in the phase plane). In Section 4, we propose a suitable characterization of the asymptotic limit ‘ $b = +\infty$ ’, in which relation $G(t) = Q(V(t))$ is imposed.

Remark: Issues of continuity

In Sections 3 and 4, we propose characterizations and formulas for two respective regimes, which we term ‘ $b = 0$ ’ and ‘ $b = +\infty$ ’. However, it should be noted that the original 2D system (14) *is not* defined properly at these bounds (for $b = 0$ it is degenerated, and for $b = +\infty$ it is naturally undefined).

The 1-dimensional systems proposed in the sequel result from simple heuristics on the behavior of the 2D system (14) when parameter b gets close to the bounds of its domain. At the moment, we have no rigorous proof

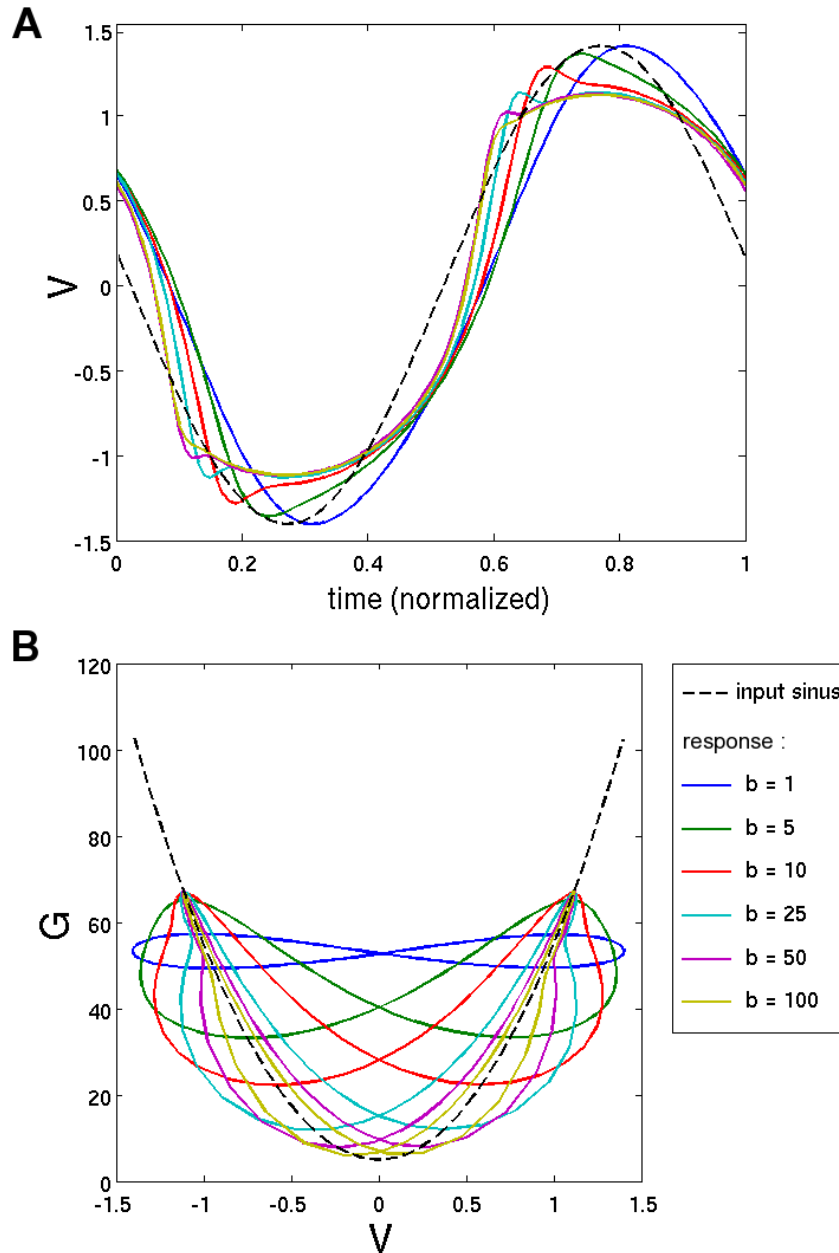


Figure 5: Response to an input sinusoidal current $I(t) = A \cos(\omega t)$, for different values of parameter b (typical frequency of the adaptation feedback). Panel A represents $V(t)$ over one period, and Panel B represents the phase portrait $(V(t), G(t))$. As b approaches the bounds of its definition domain, the system is constrained to 1D systems: ‘Flat’ system with $G(t) = \text{cst.}$ when $b \rightarrow 0$, and ‘Convex’ system with $G(t) = Q(V(t))$ when $b \rightarrow +\infty$. Other simulation parameters: $\omega = 2\pi$ Hz, $A = 75$ Hz, $Q(V) = Q_0 + \lambda V^2$ with $Q_0 = 5$ Hz and $\lambda = 50$ Hz.

of continuity between the asymptotic 2D systems (e.g. $b = \varepsilon \rightarrow 0$ and $b = 1/\varepsilon \rightarrow +\infty$) and the proposed 1D systems (' $b = 0$ ' and ' $b = +\infty$ ').

The mathematical proof of continuity may be especially problematic in the particular case $b = \varepsilon \rightarrow 0$, since as b gets close to zero, the system takes infinite time to reach its periodic asymptote (the typical time constant being $0 < \lambda_0 \leq b$).

Possible keys for a further grounding of our 1D solutions as actual limits can be found in Section 5, where we sketch some results of perturbation analysis, near $b = 0$ and $b = +\infty$. ■

3 Asymptotic behavior $b = 0$

3.1 System definition

A heuristic definition of the asymptotic system

If the asymptotic behavior for $b = 0$ is directly considered by injecting relation ' $b = 0$ ' into system (14), it yields:

$$\begin{cases} \dot{V}(t) = A \cos(\omega t) - G(t)V(t), & (a) \\ \dot{G}(t) = 0. & (b) \end{cases} \quad (28)$$

This happens to be a degenerate system, since (28-b) only indicates that $G(t) = G_0$ is a constant. In turn, (28-a) admits a valid solution for any possible value of G_0 .

A supplementary constraint must thus be found to fully define the system. And indeed, we have seen in Section 2.2.3 that once initial conditions are forgotten³, one always has $\hat{G} = \widehat{Q(V)}$, independently of b , where the hat denotes averaging over one period.

It is natural to assume that in the 'real' asymptotic limit for $b = 0$, this relation still holds, so that the only 'real' value for G_0 is the one which satisfies

$$G_0 = \widehat{Q(V)}. \quad (29)$$

In turn, if $G(t) = G_0$ is constant, equation (28-a) that drives $V(t)$ becomes linear:

$$\dot{V}(t) = A \cos(\omega t) - G_0 V(t).$$

This is a simple low-pass linear filter, whose solution we have already described in (5) and (7)-(8). We are thus able to fully express the most plausible candidate for the 'real' asymptotic value when $b = 0$.

³Which takes an infinite time as $b \rightarrow 0$! See remark at the end of the preceding section.

System definition, and proof of existence

In our asymptotic system $b = 0$, the state variable $W(t) = (V(t), G_0)$ is totally determined by a single number $G_0 > 0$, through the following hybrid system:

$$\begin{cases} V(t) = \frac{A}{\sqrt{G_0^2 + \omega^2}} \cos(\omega t - \arctan(\omega/G_0)), & (a) \\ G_0 = \frac{1}{T} \int_{u=t_0}^{t_0+T} Q(V(u)) du, & (b) \end{cases} \quad (30)$$

where t_0 can be any time, since $V(t)$ is T -periodic. The system is well defined, thanks to the following proposition.

Proposition 3 *System (30) forces a single possible value for G_0 , and thus for $W(t) = (V(t), G_0)$. Furthermore, G_0 is C^1 w.r.t. system parameters.*

Proof: Function $I(K) = \frac{1}{T} \int_{u=0}^T Q(K \cos(\omega u)) du$ is a continuous, growing function from \mathbb{R}^{+*} to $]Q_0, +\infty[$. Indeed, its derivative writes

$$I'(K) = \frac{1}{T} \int_{u=0}^T \cos(\omega t) Q'(K \cos(\omega u)) du = \frac{1}{TK} \int_{u=0}^T R(K \cos(\omega u)) du,$$

with $R(v) = vQ'(v) \geq 0$ (equation (15)).

As a result, (30-b) can rewrite $G_0 = I \circ K(G_0)$ where $K(G) = A/\sqrt{G^2 + \omega^2}$ is a decreasing function from \mathbb{R}^{+*} to $]0, A/\omega^2[$. $I \circ K$ is thus a positive decreasing function, whose graph $y = I \circ K(x)$ intersects once and only once the identity line $y = x$, defining a unique solution G_0 .

Furthermore, since functions $K(G)$ and $I(K)$ depend continuously on system parameters, so does G_0 . More precisely, for G_0 to have a C^k dependence on input parameters, it is sufficient that $v \rightarrow Q(v)$ be C^k . \square

Remark: Note that, even although equation (30-a) is obtained as the solution of a linear ODE, the whole system (30) is *not* linear with its input, since G_0 itself depends on parameters A and ω of the input current. \blacksquare

3.2 Dependence of V_{\max} and ϕ_{\max} w.r.t. system parameters

Because it has a reduced dimensionality, we are able to state precise results for system (30), concerning the dependence of V_{\max} and t_{\max} w.r.t. parameters A and ω of the input current. These results are summed up in the following theorem.

Theorem 1 *System (30) behaves as a low-pass filter with gain control on the input amplitude. First, here is how V_{\max} and ϕ_{\max} depend on input frequency ω :*

(i) *Low-pass setting*

$$\partial_\omega V_{\max} < 0 \text{ and } \lim_{\omega \rightarrow +\infty} V_{\max} = 0.$$

(ii) *Phase delay*

$$\partial_\omega \phi_{\max} > 0 \text{ and } \lim_{\omega \rightarrow +\infty} \phi_{\max} = \frac{\pi}{2} \pmod{2\pi}.$$

Second, here is how V_{\max} and ϕ_{\max} depend on input amplitude A :

(iii) *Growth of V_{\max}*

$$\partial_A V_{\max} > 0 \text{ and } \lim_{A \rightarrow +\infty} V_{\max} = +\infty.$$

(iv) *Phase advance*

$$\partial_A \phi_{\max} < 0 \text{ and } \lim_{A \rightarrow +\infty} \phi_{\max} = 0 \pmod{2\pi}.$$

(v) *Under-linearity*

$$\partial_A \frac{V_{\max}}{A} < 0 \text{ and } \lim_{A \rightarrow +\infty} \frac{V_{\max}}{A} = 0.$$

Proof:

To simplify further calculations, we express G_0 in a reduced time scale:

$$G_0 = \frac{1}{2\pi} \int_{\phi=0}^{2\pi} Q(V_{\max} \cos(\phi)) d\phi,$$

as obtained from (30-b) with the change of variable $\phi = \omega t - \arctan(\omega/G_0)$, and the choice of $t_0 = \arctan(\omega/G_0)/\omega$. Differentiating this expression w.r.t. parameter $p = A$ or ω (a valid operation thanks to Proposition 3), we get

$$\partial_p G_0 = \frac{\partial_p V_{\max}}{V_{\max}} \widehat{R(V)}, \quad (31)$$

where, again, $R(v) = vQ'(v)$ and the hat denotes average over one period.

We also remind the two expressions directly obtained from (30-a):

$$V_{\max} = A(G_0^2 + \omega^2)^{-1/2}. \quad (32)$$

$$\phi_{\max} = \arctan(\omega/G_0). \quad (33)$$

Dependence w.r.t. A (Points (iii)-(v)). Differentiation of (32) w.r.t. A yields

$$\partial_A V_{\max} = (G_0^2 + \omega^2)^{-3/2} (G_0^2 + \omega^2 - AG_0 \partial_A G_0), \quad (34)$$

which forms a coupled system with $\partial_A G_0$ (31). Solving this system provides

$$\partial_A V_{\max} = \left[\sqrt{G_0^2 + \omega^2} + \widehat{R(V)} \frac{G_0}{\sqrt{G_0^2 + \omega^2}} \right]^{-1}. \quad (35)$$

As a result, $\partial_A V_{\max} > 0$ (growth of system response with input amplitude) and $\partial_A G_0 > 0$ (with (31)). Then, because G_0 grows with A , (32) implies that $\partial_A (V_{\max}/A) < 0$ (under-linearity of system response with input amplitude), and (33) implies that $\partial_A \phi_{\max} < 0$ (phase advance with increasing amplitude).

To conclude the proof of Points (iii)-(v), we must find the respective limits of V_{\max} , ϕ_{\max} and V_{\max}/A when $A \rightarrow +\infty$. These three limits are determined by $G_\infty = \lim_{A \rightarrow +\infty} G_0 \in \mathbb{R}^+ \cup \{+\infty\}$, a number that must exist since G_0 grows with A .

Suppose $G_\infty \in \mathbb{R}$. Through (32) V_{\max} would also have a finite limit in \mathbb{R} , and necessarily $\lim_{A \rightarrow +\infty} \partial_A V_{\max} = 0$. This would be in contradiction with (35). As a result, $G_\infty = +\infty$, and (32)-(33) provide the limits stated by Points (iii)-(v).

Dependence w.r.t. ω (Points (i) and (ii)). In this case, equation (34) is replaced by

$$\partial_\omega V_{\max} = -A(G_0^2 + \omega^2)^{-3/2} (G_0 \partial_\omega G_0 + \omega). \quad (36)$$

The rest of the demonstration follows in a fashion similar to Points (iii)-(v). \square

4 Asymptotic behavior $b = +\infty$

4.1 System definition

We define our asymptotic system $b = +\infty$ as the following 1-dimensional ODE:

$$\dot{V}(t) = A \cos(\omega t) - V(t)Q(V(t)). \quad (37)$$

This system is the straightforward extension of the 2D system (14), when equation (14-b) is replaced by the asymptotic relation $G(t) = Q(V(t))$.

We will also consider the alternative formulation:

$$\dot{V}(t) = L(E(t)) - L(V(t)), \quad (38)$$

where $L(v) = vQ(v)$ is a diffeomorphism from \mathbb{R} to itself (as in (16)), and $E(t)$ defined as

$$E(t) = L^{-1}(A \cos(\omega t)) \quad (39)$$

acts as a driving potential on $V(t)$.

Remark: Letters L and E are chosen in link with their signification in a neuron membrane model. The term $L(V(t))$ in (38) is the instantaneous *Leak* current in the membrane, while $E(t)$ in (38) has the dimension of an attracting electrical potential, often noted E in neurophysiology. ■

The following Proposition insures that system (14) reaches exponentially fast a well-defined periodic solution $V(t)$ (as Proposition 1 in the 2D case). Furthermore, it states the existence of a single local maximum over each cycle.

Proposition 4

- (i) Equation (37) admits a unique T -periodic solution that we note $V(t)$. All other solutions $W(t)$ to (37) converge asymptotically fast to $V(t)$.
- (ii) $V(t)$ is $T/2$ -antiperiodic: $V(t) = -V(t + T/2)$. Over one period, $V(t)$ has a single local maximum V_{\max} reached at time t_{\max} , and a single local minimum $V_{\min} = -V_{\max}$ reached at time $t_{\min} = t_{\max} - T/2$. Furthermore, $t_{\max} \in [0, T/4] \pmod{T}$.
- (iii) Function $V : t \rightarrow V(t)$ admits C^1 differentiation w. r. t. parameter A and Gâteaux derivatives w.r.t. function Q , in the space of $T/2$ -antiperiodic functions with norm $\| \cdot \|_{\infty}$.

Proof:

The proof of all three Points relies on the same argument as Proposition 1 in the 2D case: System (37) is contracting. The whole demonstration is made in the same way⁴ and we will not repeat it here.

The only specific point left to prove here is the existence of a single local maximum in each cycle (Point (ii)). Note that this result does not hold in the general 2D case (see Figure 4). But in the present 1D system, equation (38) implies that local extrema of $V(t)$ correspond to points where $V(t)$ crosses $E(t)$.

More precisely, let us rewrite (38) and its derivative:

$$\begin{aligned}\dot{V}(s) &= L(E(s)) - L(V(s)) \\ \ddot{V}(s) &= \dot{E}(s)L'(E(s)) - \dot{V}(s)L'(V(s))\end{aligned}$$

Let s be a local maximum of V . One has $\dot{V}(s) = 0$ and $\ddot{V}(s) \leq 0$, so $V(s) = E(s)$ and $\dot{E}(s) = \ddot{V}(s)/L'(E(s)) \leq 0$. This last inequality can be made strict: Suppose $\ddot{V}(s) = 0$, then one must also

⁴Note that rigorously, results for the 2D system cannot be directly applied here, because the 2D system is not defined for $b = +\infty$.

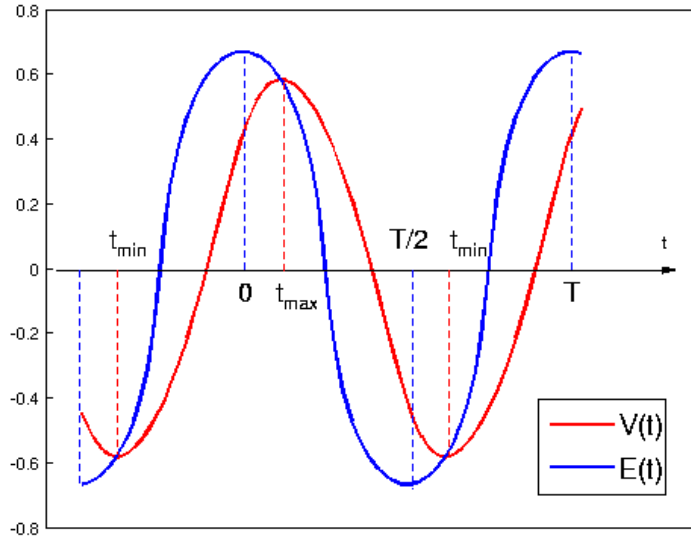


Figure 6: Driving potential $E(t) = L^{-1}(A \cos(\omega t))$, and periodic solution $V(t)$, represented for a particular set of parameters, and a quadratic leak function $Q(v) = Q_0 + \lambda v^2$.

have $\ddot{V}(s) = 0$ because s is a local extremum. So one must have at the same time $\dot{E}(s) = 0$ and $\ddot{E}(s) = 0$, which never happens.

In the end, for any time s :

$$s \text{ is a local maximum of } V \iff (V(s) = E(s) \text{ and } \dot{E}(s) < 0)$$

$$s \text{ is a local minimum of } V \iff (V(s) = E(s) \text{ and } \dot{E}(s) > 0)$$

As any continuous function⁵, $V(t)$ necessarily displays an *alternation* of local maxima and local minima. As a result, the sign of $\frac{d}{dt}E(s)$ necessarily changes between two successive extrema, and $V(t)$ can only have one local maximum t_{\max} and one local minimum $t_{\min} = t_{\max} - T/2$ per cycle. The maximum is reached in the positive descending phase of $E(t)$, with t_{\max} comprised between 0 and $T/4$ (modulo T). The minimum is reached anti-symmetrically, in the negative ascending phase of $E(t)$. This is illustrated in Figure 6. \square

Before introducing our main result (Theorem 2, Section 4.3), we state two useful propositions in the next section, which provide integral expressions for the partial derivatives $\partial_p V(t)$ in the system.

⁵save one which is locally constant...

4.2 Integral formulations for partial derivatives in the system

Proposition 5 (Integral formulation for partial derivatives)

Consider $V(t)$ the unique periodic solution of (37):

$$\dot{V}(t) = A \cos(\omega t) - L(V(t)),$$

and p a parameter of the system (e.g., A), for which $t \rightarrow \partial_p V(t)$ is well-defined. Then, for all t :

$$\partial_p V(t) = \frac{1}{1 + \exp\left(-\int_{s=t-T/2}^t L'(V(s)) ds\right)} \int_{u=t-T/2}^t Y_p(u) \exp\left(-\int_{s=u}^t L'(V(s)) ds\right) du, \quad (40)$$

with

$$Y_p(t) = \partial_p (A \cos(\omega t)) - V(t)(\partial_p Q)(V(t)),$$

and in particular:

$$\partial_p V_{\max} = \frac{1}{1 + \exp\left(-\int_{s=t_{\min}}^{t_{\max}} L'(V(s)) ds\right)} \int_{u=t_{\min}}^{t_{\max}} Y_p(u) \exp\left(-\int_{s=u}^{t_{\max}} L'(V(s)) ds\right) du. \quad (41)$$

A similar relation can be obtained if ∂_p is replaced by $\frac{d}{dt}$, or by a well-defined Gâteaux derivative for function Q along a symmetric function Q_2 .

Proof:

Differentiation of (37) leads to the following ODE on $\partial_p V(t)$:

$$\begin{aligned} \frac{d}{dt} \partial_p V(t) &= \partial_p (A \cos(\omega t)) - V(t)(\partial_p Q)(V(t)) - L'(V(t)) \partial_p V(t) \\ &= Y_p(t) - L'(V(t)) \partial_p V(t), \end{aligned}$$

with the definition for $Y_p(t)$ given in Proposition 5. This is a linear equation on function $t \rightarrow \partial_p V(t)$, so it can be integrated, starting from any initial condition t_0 :

$$\partial_p V(t) = \partial_p V(t_0) \exp\left(-\int_{s=t_0}^t L'(V(s)) ds\right) + \int_{u=t_0}^t Y_p(u) \exp\left(-\int_{s=u}^t L'(V(s)) ds\right) du. \quad (42)$$

But system (37) is $T/2$ -antiperiodic, and so is $V(t)$. So, $\partial_p V(t)$ is also $T/2$ -antiperiodic: $\partial_p V(t - T/2) = -\partial_p V(t)$. Taking $t_0 = t - T/2$ in (42) leads to expression (40).

Then, since $V_{\max} = V(t_{\max})$, we have:

$$\partial_p V_{\max} = (\partial_p V)(t_{\max}) + \dot{V}(t_{\max}) \partial_p t_{\max} = (\partial_p V)(t_{\max}), \quad (43)$$

since $\dot{V}(t_{\max}) = 0$. This proves (41). All the steps of this proof are similar if ∂_p is replaced by $\frac{d}{dt}$, or by a Gâteaux derivative for Q . \square

As a first application of Proposition 5, we present a proposition concerning the influence of the leak function Q on system (37). This proposition can be considered as a result by itself. Furthermore, we will use the calculations made here to prove Theorem 2 (Section 4.3).

Proposition 6 (Gâteaux derivative for leak function Q)

Consider $V(t)$ the unique periodic solution of (37):

$$\dot{V}(t) = A \cos(\omega t) - L(V(t)).$$

Let $v \rightarrow Q_2(v)$ be an even function with sufficient regularity, and such that $V(t)$ admits a Gâteaux derivative $\partial_Q^{(Q_2)} V(t)$ when the leak function Q is modified along Q_2 . Then:

(i) The variation of V_{\max} (maximum of $V(t)$) is given by:

$$\partial_Q^{(Q_2)} V_{\max} = -\frac{V_{\max} Q_2(V_{\max})}{L'(V_{\max})} + \frac{\int_{u=t_{\min}}^{t_{\max}} \frac{d}{dv} \left[\frac{v Q_2(v)}{L'(v)} \right] (V(u)) \dot{V}(u) \exp \left(-\int_u^{t_{\max}} L'(V) \right) du}{\left(1 + \exp \left(-\int_{t_{\min}}^{t_{\max}} L'(V) \right) \right)}.$$
(44)

(ii) The variation of t_{\max} (time for the maximum of $V(t)$) is given by:

$$\partial_Q^{(Q_2)} t_{\max} = -\frac{L'(V_{\max})}{A\omega \sin(\omega t_{\max})} \cdot \frac{\int_{u=t_{\min}}^{t_{\max}} \frac{d}{dv} \left[\frac{v Q_2(v)}{L'(v)} \right] (V(u)) \dot{V}(u) \exp \left(-\int_u^{t_{\max}} L'(V) \right) du}{\left(1 + \exp \left(-\int_{t_{\min}}^{t_{\max}} L'(V) \right) \right)}.$$
(45)

(iii) Generally, one has a time advance for increased leak: To have $\partial_Q^{(Q_2)} t_{\max} < 0$, a sufficient condition is that $Q_2(v)$ verifies:

$$\forall v, \quad \frac{d}{dv} \left[\frac{v Q_2(v)}{L'(v)} \right] > 0.$$

In (i)-(iii), notation $\frac{d}{dv} [\]$ denotes derivation of the function inside with respect to v . The expression $\int L'(V)$ stands for $\int L'(V(s)) ds$.

Proof:

Let us start by expressing $\partial_Q^{(Q_2)} V$ in the integral formulation of Proposition 5. When relation $\dot{V}(t) = A \cos(\omega t) - L(V(t))$ is differentiated along Q_2 , it yields:

$$\frac{d}{dt} \partial_Q^{(Q_2)} V(t) = -V(t)Q_2(V(t)) - L'(V(t))\partial_Q^{(Q_2)} V(t). \quad (46)$$

The first term of the right-hand side is the Gâteaux derivative w.r.t. Q_2 of function $v \rightarrow L(v) = vQ(v)$, while the second term is the variation of $L(V(t))$ due to $\partial_Q^{(Q_2)} V(t)$. Applying formula (41) from Proposition 5 yields:

$$\begin{aligned} & \left(1 + \exp\left(-\int_{t_{\min}}^{t_{\max}} L'(V)\right)\right) \partial_Q^{(Q_2)} V_{\max} \\ &= -\int_{u=t_{\min}}^{t_{\max}} V(u)Q_2(V(u)) \exp\left(-\int_u^{t_{\max}} L'(V)\right) du \\ &= -\int_{u=t_{\min}}^{t_{\max}} \frac{V(u)Q_2(V(u))}{L'(V(u))} L'(V(u)) \exp\left(-\int_u^{t_{\max}} L'(V)\right) du \\ &= -\left[\frac{V(u)Q_2(V(u))}{L'(V(u))} \exp\left(-\int_u^{t_{\max}} L'(V)\right)\right]_{t_{\min}}^{t_{\max}} \\ & \quad + \int_{u=t_{\min}}^{t_{\max}} \left(\frac{d}{dt} \frac{VQ_2(V)}{L'(V)}\right)(u) \exp\left(-\int_u^{t_{\max}} L'(V)\right) du \\ &= -\left(1 + \exp\left(-\int_{t_{\min}}^{t_{\max}} L'(V)\right)\right) \frac{V_{\max}Q_2(V_{\max})}{L'(V_{\max})} \\ & \quad + \int_{u=t_{\min}}^{t_{\max}} \left[\frac{vQ_2(v)}{L'(v)}\right]'(V(u)) \dot{V}(u) \exp\left(-\int_u^{t_{\max}} L'(V)\right) du, \end{aligned}$$

using an integration by parts from line 3 to 4. From line 4 to last, we use the fact that $V(t_{\min}) = -V_{\max}$, and Q_2 and L' are even functions. Dividing the last line by $(1 + \exp(-\int_{t_{\min}}^{t_{\max}} L'(V)))$ yields Point (i) of the Proposition.

Now from another point of view, remark that $V(t)$ and driving potential $E(t)$ coincide at time t_{\max} , so we have:

$$\begin{aligned} V_{\max} &= E(t_{\max}) \\ \partial_Q^{(Q_2)} V_{\max} &= (\partial_Q^{(Q_2)} E)(t_{\max}) + \partial_Q^{(Q_2)} t_{\max} \dot{E}(t_{\max}). \end{aligned} \quad (47)$$

To calculate the right-hand side term, we differentiate relation $L(E(t)) = A \cos(\omega t)$ in two different ways: First along t , second along Q_2 . It yields

$$\begin{aligned} \dot{E}(t)L'(E(t)) &= -\omega A \sin(\omega t), \\ (\partial_Q^{(Q_2)} E)(t)L'(E(t)) + E(t)Q_2(E(t)) &= 0. \end{aligned}$$

The corresponding values for $\dot{E}(t_{\max})$ and $(\partial_Q^{(Q_2)} E)(t_{\max})$ can be deduced and injected into (47), yielding:

$$\partial_Q^{(Q_2)} V_{\max} = -\frac{V_{\max} Q_2(V_{\max})}{L'(V_{\max})} - \partial_Q^{(Q_2)} t_{\max} \frac{\omega A \sin(\omega t_{\max})}{L'(V_{\max})}. \quad (48)$$

Equations (44) and (48) provide two different expressions for $\partial_Q^{(Q_2)} V_{\max}$. By subtracting them, one gets the expression for $\partial_Q^{(Q_2)} t_{\max}$ proposed in Point (ii) of the Proposition.

To prove Point (iii), simply remark that if $[\frac{vQ_2(v)}{L'(v)}]' > 0$ for all v , then the integral in Point (ii) becomes trivially positive (since $\dot{V}(u) \geq 0$ over $[t_{\min}, t_{\max}]$), implying $\partial_Q^{(Q_2)} t_{\max} < 0$. \square

To illustrate this result, we give below two examples of application of Proposition 6, for different expressions of the leak functions Q .

Example 1: Constant leak function

If $Q(v) = Q_0$ and $Q_2(v) = 1$ are taken as constant functions, system (37) becomes the simple linear exponential filter (4), with time constant $1/Q_0$. In this case, Point (iii) can simply be reinterpreted as $\partial_{Q_0} t_{\max} < 0$, coherently with well-known results for the linear exponential filter. \blacksquare

Example 2: Quadratic leak function

To get more insight on the condition $[vQ_2(v)/L'(v)]' > 0$, required by Point (iii) of the Proposition, let us consider a function Q of the form

$$Q(v) = a + \lambda v^2.$$

First, if we take $Q_2(v) = v^2$, the Gâteaux derivative along Q_2 amounts to a partial derivative when parameter λ is modified. And one has

$$[vQ_2(v)/L'(v)]' = [v^3/(a + 3\lambda v^2)]' = (3av^2 + 3\lambda v^4)/(a + 3\lambda v^2)^2 > 0,$$

meaning that $\partial_\lambda t_{\max} < 0$.

By opposition, if we take $Q_2(v) = 1$, the Gâteaux derivative along Q_2 amounts to a partial derivative when parameter a is modified. But there:

$$[vQ_2(v)/L'(v)]' = [v/(a + 3\lambda v^2)]' = (a - 3\lambda v^2)/(a + 3\lambda v^2)^2,$$

so Point (iii) *does not* apply. And indeed, numerical simulations (under Matlab) often reveal that as a augments, t_{\max} undergoes important fluctuations, and is highly non-monotonic with a .

The non-monotony of t_{\max} with a can be explained by the following heuristic argument: When the static leak a augments, it tends to make V_{\max} smaller, and thus the mean value of λV^2 gets smaller, which somehow compensates for the augmentation of a in the total leak $Q(V(t)) = a + \lambda V(t)^2$. ■

4.3 Dependence of V_{\max} and ϕ_{\max} w.r.t. system parameters

Because it has a reduced dimensionality, we are able to state precise results for system (37), concerning the dependence of V_{\max} and t_{\max} w.r.t. parameters A and ω of the input current. These results are summed up in the following theorem.

Theorem 2 *System (37) behaves as a low-pass filter with gain control on the input amplitude. First, here is how V_{\max} and ϕ_{\max} depend on input frequency ω :*

(i) *Low-pass setting*

$$\partial_{\omega} V_{\max} < 0 \text{ and } \lim_{\omega \rightarrow +\infty} V_{\max} = 0.$$

(ii) *Phase delay*

$$\partial_{\omega}(\phi_{\max}) > 0 \text{ and } \lim_{\omega \rightarrow +\infty} \phi_{\max} = \frac{\pi}{2} \pmod{2\pi}.$$

Second, here is how V_{\max} and ϕ_{\max} depend on the amplitude A :

(iii) *Growth of V_{\max}*

$$\partial_A V_{\max} > 0 \text{ and } \lim_{A \rightarrow +\infty} V_{\max} = +\infty.$$

(iv) *Phase advance*

$$\partial_A \phi_{\max} < 0 \text{ and } \lim_{A \rightarrow +\infty} \phi_{\max} = 0 \pmod{2\pi}.$$

(v) *Under-linearity*

$$\forall (\omega, Q), \text{ if } A \text{ is high enough, } \partial_A \frac{V_{\max}}{A} < 0.$$

$$\text{Also, } \lim_{A \rightarrow +\infty} \frac{V_{\max}}{A} = 0.$$

(vi) *Asymptotic equivalents*

$$V_{\max} \underset{A \rightarrow +\infty}{\sim} L^{-1}(A), \text{ and } \partial_A V_{\max} \underset{A \rightarrow +\infty}{\sim} \frac{1}{L'(V_{\max})}.$$

This theorem has the same form as Theorem 1 in the case $b = 0$, except for two details. First, there is an additional Point (vi) concerning equivalents for V_{\max} when $A \rightarrow +\infty$. Its results are more powerful than the simple asymptotic limits given in Points (iii) and (v).

Second, the under-linearity of V_{\max} w.r.t. A , stated in Point (v), also differs from Theorem 1 because we prove that $\partial_A(V_{\max}/A) < 0$ only asymptotically (if A is big enough). We were not able to fully prove that $\partial_A(V_{\max}/A) < 0$ for any set of parameters.

Experimentally, we always found the relation $\partial_A(V_{\max}/A) < 0$ to be true. Proposition 7 in Section 4.4 gives a non-differential equivalent to assertion $\partial_A(V_{\max}/A) < 0$, and provides a sufficient condition to have this inequality verified.

Proof:

We first demonstrate relations related to A (Points (iii)-(vi), Section 4.3.1), and then relations related to ω (Points (i)-(ii), Section 4.3.2), which are simpler and based on similar ideas. In both cases, it is convenient to first demonstrate all signs of variation of the form $\partial_p X$, and afterward to compute all the corresponding limits $\lim_{p \rightarrow +\infty} X$.

4.3.1 Dependence w.r.t. A (Points (iii)-(vi)).

Signs of variation

To prove $\partial_A V_{\max} > 0$, we use the integral formulation from Proposition 5. In this case, one has $Y_A(t) = \cos(\omega t)$, so (41) provides the formula:

$$\partial_A V_{\max} = \frac{1}{1 + \exp\left(-\int_{t_{\min}}^{t_{\max}} L'(V)\right)} \int_{u=t_{\min}}^{t_{\max}} \cos(\omega u) \exp\left(-\int_u^{t_{\max}} L'(V)\right) du. \quad (49)$$

One can easily get convinced that this integral is always positive (see Figure 7). Indeed, interval $[t_{\min}, -T/4]$, on which $\cos(\omega u)$ is negative, is smaller than interval $[-T/4, t_{\max}]$ on which $\cos(\omega u)$ is positive. Furthermore, function $u \rightarrow \exp(-\int_u^{t_{\max}} L'(V(s))ds)$ is a positive growing function (schematically represented in green in Figure 7), that enhances even more the positive contribution of the cosine as compared to the negative contribution. As a result, one has indeed $\partial_A V_{\max} > 0$.

To prove $\partial_A \phi_{\max} < 0$, first note that

$$\partial_A \phi_{\max} = \partial_A(\omega t_{\max}) = \omega \partial_A t_{\max},$$

so we can rather focus on proving $\partial_A t_{\max} < 0$. Let us introduce the reduced variable

$$U(t) = \frac{V(t)}{A}, \quad (50)$$

which is governed by the following ODE :

$$\dot{U}(t) = \cos(\omega t) - U(t)Q(AU(t)). \quad (51)$$

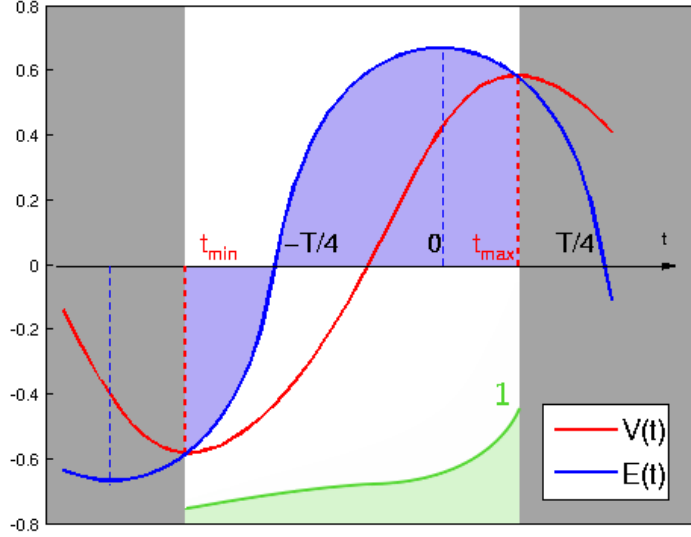


Figure 7: Zoom on $E(t)$ and $V(t)$ from t_{\min} to t_{\max} . The blue zone is a schematic view of the integral of $\cos(\omega u)$ over this interval. The green curve is a schematic view of function $u \rightarrow \exp(-\int_u^{t_{\max}} L'(V(s))ds)$, a growing function reaching value 1 in $u = t_{\max}$.

$U(t)$ is driven by an equation of the same nature as (37), except that its leak function is $Q_A : u \rightarrow Q(Au)$, having A as an internal parameter. Naturally, time t_{\max} also corresponds to the maximum of $U(t)$. Now, remark that for an infinitesimal $\varepsilon > 0$:

$$\begin{aligned} Q((A + \varepsilon)u) &= Q(Au) + \varepsilon u Q'(Au) + o(\varepsilon) \\ &= (Q + \varepsilon Q_2)(Au) + o(\varepsilon), \end{aligned}$$

with

$$Q_2(v) = \frac{vQ'(v)}{A} = \frac{R(v)}{A}.$$

So, from the point of view of system (51) on $U(t)$, a perturbation $A + \varepsilon$ has the same effect as replacing function Q by function $Q + \varepsilon Q_2$. This implies:

$$\partial_A t_{\max} = \partial_Q^{(Q_2)} t_{\max} = \frac{1}{A} \partial_Q^{(R)} t_{\max}. \quad (52)$$

We can then directly apply the results of Proposition 6, concerning Gâteaux derivatives. Indeed, function $v \rightarrow \frac{vR(v)}{L'(v)}$ is a growing function of v . Its derivative writes (we only provide the result):

$$\frac{d}{dv} \left[\frac{vR(v)}{L'(v)} \right] = \frac{2R(v)Q(v) + v^2Q''(v)}{L'(v)^2}, \quad (53)$$

which is positive because Q is convex ($Q''(v) \geq 0$). As a result, Point (iii) of Proposition 6 allows to directly conclude: $\partial_A t_{\max} < 0$, as stated by Point (iv) of the Theorem.

Remark: Naturally, this result could also be obtained without using Gâteaux derivatives, by direct differentiation of (51) along A , and calculations similar to the proof of Proposition 6. ■

Limits

We can now find the associated limits in Points (iii)-(v). Let us note $\phi_{\max} = \omega t_{\max}$ modulo 2π (so that $\phi_{\max} \in]0, \pi/2[$), and denote $\phi_{\infty} \geq 0$ the limit of ϕ_{\max} when $A \rightarrow +\infty$. We know this limit exists because we have just proved $\partial_A t_{\max} < 0$.

First, note that $L(V_{\max}) = A \cos(\phi_{\max})$. Since $\cos(\phi_{\infty}) > 0$, this implies

$$V_{\max} \underset{A \rightarrow +\infty}{\sim} L^{-1}(A \cos(\phi_{\infty})). \quad (54)$$

So, $\lim_{A \rightarrow +\infty} V_{\max} = +\infty$ and Point (iii) is proved. Also, since $L^{-1}(v)$ is under-linear, one has $\lim_{A \rightarrow +\infty} (V_{\max}/A) = 0$, as stated by Point (iv). Equation (54) will also provide the first asymptotic result in Point (v), once we show that $\phi_{\infty} = 0$.

To prove that $\phi_{\infty} = 0$, integrate the driving equation $\dot{V}(t) = A \cos(\omega t) - L(V)$ between $-t_{\max}$ and t_{\max} :

$$V_{\max} - V(-t_{\max}) = \int_{-t_{\max}}^{t_{\max}} (A \cos(\omega t) - L(V(t))) dt. \quad (55)$$

The integral on the right-hand side of (55) is schematically represented in Figure 8, in color *green*. Since function $t \rightarrow \cos(\omega t)$ is concave over $[-t_{\max}, t_{\max}]$, the integral term in (55) is bigger than the triangular area depicted in black *red* in Figure 8. Which writes:

$$\int_{-t_{\max}}^{t_{\max}} (A \cos(\omega t) - L(V(t))) dt \geq t_{\max} (A - L(V_{\max})).$$

And since, trivially, $V_{\max} - V(-t_{\max}) \leq 2V_{\max}$, equation (55) implies the inequality:

$$2V_{\max} \geq t_{\max} (A - L(V_{\max})). \quad (56)$$

Now suppose that $\phi_{\infty} > 0$. In that case, (56) would imply that

$$2 \liminf_{A \rightarrow +\infty} V_{\max} \geq A \frac{\phi_{\infty}}{\omega} (1 - \cos(\phi_{\infty})), \quad (57)$$

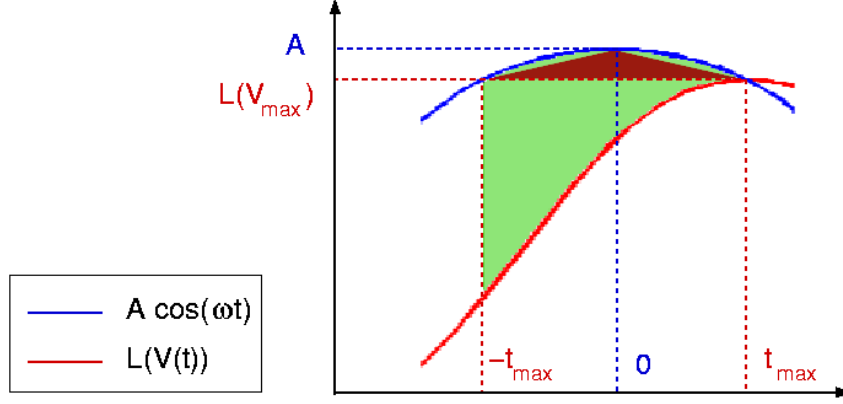


Figure 8: Functions $A \cos(\omega t)$ and $L(V(t))$, on interval $[-t_{\max}, t_{\max}]$. The integral $\int_{-t_{\max}}^{t_{\max}} (A \cos(\omega t) - L(V(t))) dt$, in green, can be minored by the area of the dark red triangle.

because of (54), and the facts that $\phi_{\infty} > 0$ and $\cos(\phi_{\infty}) < 1$. But this is in contradiction with the fact that $\lim_{A \rightarrow +\infty} (V_{\max}/A) = 0$, as resulting from (54). So $\phi_{\infty} = 0$, which concludes the proof of Point (iv).

Equivalence relations

We finish by proving the equivalence relations in Point (vi). First, since $\phi_{\infty} = 0$, equation (54) gives us the stated equivalent to V_{\max} . Then, proceed to an integration by parts starting from (49):

$$\begin{aligned}
 & \left(1 + \exp\left(-\int_{t_{\min}}^{t_{\max}} L'(V)\right)\right) \partial_A V_{\max} \\
 &= \int_{u=t_{\min}}^{t_{\max}} \frac{\cos(\omega u)}{L'(V(u))} L'(V(u)) \exp\left(-\int_u^{t_{\max}} L'(V)\right) du \\
 &= \left(1 + \exp\left(-\int_{t_{\min}}^{t_{\max}} L'(V)\right)\right) \frac{\cos(\omega t_{\max})}{L'(V_{\max})} - \int_{u=t_{\min}}^{t_{\max}} \left(\frac{d}{dt} \frac{\cos(\omega t)}{L'(V(t))}\right)(u) \exp\left(-\int_u^{t_{\max}} L'(V)\right) du,
 \end{aligned}$$

using the fact that $\cos(\omega t_{\min}) = -\cos(\omega t_{\max})$ for the first term of the sum. And so

$$\partial_A V_{\max} = \frac{\cos(\phi_{\max})}{L'(V_{\max})} - \frac{\int_{u=t_{\min}}^{t_{\max}} \left(\frac{d}{dt} \frac{\cos(\omega t)}{L'(V(t))}\right)(u) \exp\left(-\int_u^{t_{\max}} L'(V)\right) du}{1 + \exp\left(-\int_{t_{\min}}^{t_{\max}} L'(V)\right)}. \quad (58)$$

We wish to prove that when $A \rightarrow +\infty$, $\partial_A V_{\max}$ is equivalent to the first term of the right-hand side in (58), itself equivalent to $1/L'(V_{\max})$ since $\phi_\infty = 0$. First, let us admit the simple convergence relation:

$$\forall t \in [t_{\min}, t_{\max}[, F(t) = \exp\left(-\int_t^{t_{\max}} L'(V)\right) \xrightarrow{A \rightarrow +\infty} 0, \quad (59)$$

which is intuitive since $L'(V_{\max}) \rightarrow +\infty$ when $A \rightarrow +\infty$. Proving rigorously this relation is tedious.

Then, prove that the second term on the right-hand side of (58) is a $o(1/L'(V_{\max}))$:

$$\begin{aligned} & L'(V_{\max}) \frac{\int_{u=t_{\min}}^{t_{\max}} \left(\frac{d}{dt} \frac{\cos(\omega t)}{L'(V(t))}\right)(u) \exp\left(-\int_u^{t_{\max}} L'(V)\right) du}{1 + \exp\left(-\int_{t_{\min}}^{t_{\max}} L'(V)\right)} \\ & \underset{A \rightarrow +\infty}{\sim} \int_{u=t_{\min}}^{t_{\max}} L'(V_{\max}) \left(\frac{d}{dt} \frac{\cos(\omega t)}{L'(V(t))}\right)(u) F(u) du \xrightarrow{A \rightarrow +\infty} 0. \end{aligned}$$

where $F(t)$ is defined in (59). The limit comes from the fact that $F(t)$ converges simply to 0, and the integral term is dominated by

$$\int_{u=t_{\min}}^{t_{\max}} L'(V_{\max}) \left(\frac{d}{dt} \frac{\cos(\omega t)}{L'(V(t))}\right)(u) du = 2 \cos(\omega t_{\max}) < 2.$$

We thus found:

$$\partial_A V_{\max} \underset{A \rightarrow +\infty}{\sim} 1/L'(V_{\max}),$$

which finishes to prove Point (vi). But then,

$$\partial_A \frac{V_{\max}}{A} = \frac{A \partial_A V_{\max} - V_{\max}}{A^2} \underset{A \rightarrow +\infty}{\sim} \frac{L(V_{\max})/L'(V_{\max}) - V_{\max}}{A^2} = \frac{-V_{\max}^2 Q'(V_{\max})}{L'(V_{\max}) A^2},$$

using $L(v) = vQ(v)$ and $L'(v) = Q(v) + vQ'(v)$. This last result, which can also be found directly from (64), proves that $\partial_A \frac{V_{\max}}{A}$ becomes negative for A big enough. This concludes point (v) of the theorem.

4.3.2 Dependence w.r.t. ω (Points (i)-(ii))

The following results concern the dependence with respect to ω . They use similar arguments as Points (iii)-(v), with the supplementary problem that derivatives w.r.t. ω for $V(t)$ are ill-defined, because changing ω changes the period of the whole system. To solve this problem, we express our system in coordinates that make the period independent of ω : Set

$$\phi = \omega t,$$

and the system becomes ruled by:

$$\frac{d}{d\phi} V(\phi) = \frac{A}{\omega} \cos(\phi) - \frac{V(\phi)Q(V(\phi))}{\omega}. \quad (60)$$

Remark: This modification, although benign, makes notations and differentiations a bit more confusing (at least to us...). However, the underlying calculations are rather simpler here than for the amplitude-related differentiations of Points (iii)-(v). This simplicity reflects the fact that our gain control system (37) is the straightforward extension of a linear low-pass system. ■

Signs of variation

Differentiating (60) w.r.t ω leads to the following ODE:

$$\begin{aligned} \frac{d}{d\phi} (\partial_\omega V)(\phi) &= -\frac{A}{\omega^2} \cos(\phi) + \frac{L(V(\phi))}{\omega^2} - \frac{1}{\omega} L'(V(\phi)) \partial_\omega V(\phi) \\ &= -\frac{1}{\omega} \frac{d}{d\phi} V(\phi) - \frac{1}{\omega} L'(V(\phi)) \partial_\omega V(\phi), \end{aligned}$$

with $L(v) = vQ(v)$. We can again use Proposition 5 to obtain:

$$\begin{aligned} \partial_\omega V_{\max} &= \frac{1}{1 + \exp\left(-\int_{\phi_{\min}}^{\phi_{\max}} \frac{L'(V)}{\omega} d\phi\right)} \int_{\phi=\phi_{\min}}^{\phi_{\max}} \left(-\frac{1}{\omega} \frac{d}{d\phi} V(f)\right) \exp\left(-\int_{\phi}^{\phi_{\max}} \frac{L'(V)}{\omega}\right) d\phi \\ &= -\frac{1}{\omega} \frac{1}{1 + \exp\left(-\int_{t_{\min}}^{t_{\max}} L'(V)\right)} \int_{u=t_{\min}}^{t_{\max}} \dot{V}(u) \exp\left(-\int_u^{t_{\max}} L'(V)\right) du, \end{aligned}$$

where we have switched back to regular coordinates in the last line. Since \dot{V} is positive on the interval $[t_{\min}, t_{\max}]$, this formula proves $\partial_\omega V_{\max} < 0$.

Relation $\partial_\omega \phi_{\max} > 0$ can be proved without extra calculations, by using previous results. Consider a perturbation on the frequency: $\omega \rightarrow \omega + \varepsilon$. After first-order approximation of $1/(\omega + \varepsilon)$, we find that (60) is modified as follows:

$$\frac{d}{d\phi} V(\phi) = \frac{A(1 - \varepsilon/\omega)}{\omega} \cos(\phi) - \frac{VQ(V)(1 - \varepsilon/\omega)}{\omega} + o(\varepsilon). \quad (61)$$

As a result, the first-order perturbation on ϕ_{\max} induced by $\omega \rightarrow \omega + \varepsilon$ is the same as the first order perturbation induced by the simultaneous changes:

$$\begin{aligned} A &\rightarrow A - \frac{\varepsilon}{\omega} A \\ \text{and } Q(v) &\rightarrow Q(v) - \frac{\varepsilon}{\omega} Q(v). \end{aligned}$$

This writes:

$$\begin{aligned}\partial_\omega \phi_{\max} &= -\frac{A}{\omega} \partial_A \phi_{\max} - \frac{1}{\omega} \partial_Q^{(Q)} \phi_{\max} \\ &= -A \partial_A t_{\max} - \partial_Q^{(Q)} t_{\max} \\ &= -\partial_Q^{(Q+R)} t_{\max},\end{aligned}$$

because we know from (52) that $\partial_A t_{\max} = \partial_Q^{(R)} t_{\max}/A$. So in the end, since $L' = Q + R$:

$$\partial_\omega \phi_{\max} = -\partial_Q^{(L')} t_{\max}. \quad (62)$$

We then use Proposition 6 on Gâteaux derivatives, with $Q_2(v) = L'(v)$. Trivially,

$$\frac{d}{dv} [vQ_2(v)/L'(v)] = \frac{d}{dv} [v] = 1 > 0,$$

so that Point (iii) of Proposition 6 applies, and $\partial_\omega \phi_{\max} > 0$.

Limits

Finally, we find the associated limits for V_{\max} and ϕ_{\max} when $\omega \rightarrow +\infty$. Let us integrate (60) between $\phi_{\min} = \phi_{\max} - \pi$ and ϕ_{\max} :

$$\begin{aligned}2V_{\max} &= \frac{2A \sin(\phi_{\max})}{\omega} - \int_{\phi_{\min}}^{\phi_{\max}} \frac{L(V(\phi))}{\omega} d\phi \\ &\leq \frac{2A}{\omega} + \frac{\pi A}{\omega} \\ V_{\max} &\leq \frac{A(1 + \pi/2)}{\omega},\end{aligned}$$

where the integral term was majored using $|L(V)| \leq A$. So $\lim_{\omega \rightarrow +\infty} V_{\max} = 0$, and since $L(V_{\max}) = A \cos(\phi_{\max})$, $\lim_{\omega \rightarrow +\infty} \phi_{\max} = \pi/2$. This concludes the proof of the theorem. \square

4.4 Local under-linearity of V_{\max} w.r.t. A

To conclude this presentation of the asymptotic system $b = +\infty$, we present our tentative to show that the system is always locally under-linear with input amplitude:

$$\partial_A (V_{\max}/A) < 0.$$

This result would complete Theorem 2, by making the local variation property in Point (v) true for all A , and not only for A high enough.

Although we did not manage to prove that this relation is always true, we could find a simpler, and more intuitive equivalence to the relation. Using this equivalence, we could state a sufficient condition for $\partial_A (V_{\max}/A) < 0$ to be true.

Proposition 7 (Local under-linearity of V_{\max} w.r.t. A)

Consider $V(t)$ the unique periodic solution of (37):

$$\dot{V}(t) = A \cos(\omega t) - L(V(t)).$$

Then:

$$(i) \quad \partial_A \frac{V_{\max}}{A} < 0 \Leftrightarrow \begin{cases} \int_{u=t_{\min}}^{t_{\max}} \left[\frac{v^2 Q'(v)}{L'(v)} \right]' (V(u)) \dot{V}(u) \exp \left(- \int_u^{t_{\max}} L'(V) \right) du \\ < \frac{V_{\max}^2 Q'(V_{\max})}{L'(V_{\max})} \left(1 + \exp \left(- \int_{t_{\min}}^{t_{\max}} L'(V) \right) \right) \end{cases}$$

(ii) A sufficient condition to have $\partial_A \frac{V_{\max}}{A} < 0$ is that the following, even function:

$$H(v) = \exp \left(- \int_{T(v)}^{t_{\max}} L'(V(s)) ds \right) + \exp \left(- \int_{T(-v)}^{t_{\max}} L'(V(s)) ds \right) \quad (63)$$

have its maximum over $[0, V_{\max}]$ reached in $v = V_{\max}$.

We have noted $T(v) : [-V_{\max}, V_{\max}] \rightarrow [t_{\min}, t_{\max}]$ the reciprocal function of $V(t)$ over $[t_{\min}, t_{\max}]$.

Point (i) allowed us to test under Matlab, in a simple fashion, whether or not $\partial_A \frac{V_{\max}}{A} < 0$ was true for the given set of parameters. We always found the inequality in Point (i) to be true.

Point (ii) states a sufficient condition for which the inequality in Point (i) can be easily proved true. We tried to prove this sufficient condition, but did not manage. Under simulation with Matlab, the sufficient condition was found true in all simulations, except when A was taken very close to zero (with value around $10^{-3}\omega$). But in these cases, $H(v) \simeq 2$ for all v , and at the same time Matlab calculated a whole period of $V(t)$ with less than ten sample points. So the exceptions found in these particular cases could very possibly be due to numerical imprecision.

Remark that the condition enunciated in Point (ii) appears plausible. The function

$$v \rightarrow \exp \left(- \int_{T(v)}^{t_{\max}} L'(V(s)) ds \right)$$

decreases exponentially as v gets away from V_{\max} . So, from the moment that $L'(V(s))$ takes relatively large values, both terms in $H(v)$ become very small, unless v is close to V_{\max} .

We proved that, whatever set of parameters, V_{\max} is a *local* maximum for $H(v)$, because $H'(v) > 0$ near V_{\max} . More precisely, one has

$$H(V_{\max}) - H(V_{\max} - \varepsilon) = \sqrt{\frac{2}{A\omega \sin(\omega t_{\max})}} L'(V_{\max}) \left(1 - \exp \left(- \int_{t_{\min}}^{t_{\max}} L'(V) \right) \right) \varepsilon^{1/2} + o(\varepsilon^{1/2}),$$

so that $\lim_{v \rightarrow V_{\max}} H'(v) = +\infty$. This asymptotic relation is not proved here.

Proof of Proposition 7

Point (i) comes from the fact that

$$\partial_A \frac{V_{\max}}{A} = \frac{1}{A^2} \partial_Q^{(R)} V_{\max}, \quad (64)$$

with $R(v) = vQ'(v)$, a result proved exactly as (52). The expression of $\partial_Q^{(R)} V_{\max}$ is given by equation (44) of Proposition 6. Solving $\partial_A \frac{V_{\max}}{A} < 0$ then yields the inequality in Point (i).

To prove Point (ii), we re-express the integral term in Point (i) in terms of variable V rather than t , by using the reciprocal function $T(v)$. We get:

$$\begin{aligned} F &= \int_{u=t_{\min}}^{t_{\max}} \frac{d}{dv} \left[\frac{v^2 Q'(v)}{L'(v)} \right] (V(u)) \dot{V}(u) \exp \left(- \int_u^{t_{\max}} L' \right) du \\ &= \int_{V=-V_{\max}}^{V_{\max}} \frac{d}{dv} \left[\frac{v^2 Q'(v)}{L'(v)} \right] (V) \exp \left(- \int_{T(V)}^{t_{\max}} L' \right) dV \\ &= \int_{V=0}^{V_{\max}} \frac{d}{dv} \left[\frac{v^2 Q'(v)}{L'(v)} \right] (V) \left(\exp \left(- \int_{T(V)}^{t_{\max}} L' \right) + \exp \left(- \int_{T(-V)}^{t_{\max}} L' \right) \right) dV \\ &= \int_{V=0}^{V_{\max}} \frac{d}{dv} \left[\frac{v^2 Q'(v)}{L'(v)} \right] (V) H(V) dV \end{aligned} \quad (65)$$

by symmetry of function $\frac{d}{dv} \left[\frac{v^2 Q'(v)}{L'(v)} \right]$. If the hypothesis $\forall v, H(v) \leq H(V_{\max})$ is verified, and since $\frac{d}{dv} \left[\frac{v^2 Q'(v)}{L'(v)} \right] > 0$ as proved before in (53), relation (65) can be continued into:

$$\begin{aligned} F &< H(V_{\max}) \int_{V=0}^{V_{\max}} \frac{d}{dv} \left[\frac{v^2 Q'(v)}{L'(v)} \right] (V) dV \\ F &< \left(1 + \exp \left(- \int_{t_{\min}}^{t_{\max}} L'(V) \right) \right) \frac{V_{\max}^2 Q'(V_{\max})}{L'(V_{\max})}, \end{aligned}$$

which is precisely the equivalence condition stated in Point (i). \square

5 A track for the future: Perturbation analysis

To conclude this chapter, we report some preliminary results when perturbation analysis is applied near the boundaries of b 's domain of definition: $b \rightarrow 0$ and $b \rightarrow +\infty$.

The base assumption (verified experimentally) is that the 1D systems $b = 0$ and $b = +\infty$ presented in the preceding sections constitute natural *continuous* limits of the 2D system (14), so

that the following expansion can be written:

$$\begin{cases} V^{(\varepsilon)}(t) = V_0(t) + \varepsilon V_1(t) + \cdots + \varepsilon^k V_k(t) + o(\varepsilon^k), \\ G^{(\varepsilon)}(t) = G_0(t) + \varepsilon G_1(t) + \cdots + \varepsilon^k G_k(t) + o(\varepsilon^k), \end{cases} \quad (66)$$

where:

- $(V_0(t), G_0(t))$ is the asymptotic 1D-system $b = 0$ (resp. $b = +\infty$).
- $(V^{(\varepsilon)}(t), G^{(\varepsilon)}(t))$ is the solution of 2D system (14) for parameter $b = b(\varepsilon)$, where $\varepsilon > 0$ and $b(\varepsilon)$ is a well-chosen decreasing (resp. increasing) function such that $\lim_{\varepsilon \rightarrow 0^+} b(\varepsilon) = 0$ (resp. $+\infty$).
- The coefficients $(V_k(t), G_k(t))$ of the expansion exist if and only if function $\varepsilon \rightarrow V^{(\varepsilon)}(t)$ admits a C^k extension in $\varepsilon = 0$.

In this section, we limit ourselves to C^1 expansions. We assume that a C^1 expansion is well defined in $b = 0$ for function $b(\varepsilon) = \varepsilon$, and in $b = +\infty$ for function $b(\varepsilon) = \varepsilon^{-1}$, and derive results from this assumption⁶.

We start by presenting the expansion near $b = +\infty$ (Section 5.1), which provides simpler calculations and higher hopes of generalization to the k -th order. We then present the expansion near $b = 0$ (Section 5.2).

5.1 Perturbation analysis near $b \rightarrow +\infty$

The simplest function $b(\varepsilon)$ tending to $+\infty$ is obviously $b(\varepsilon) = \varepsilon^{-1}$, and the consistency of the following results suggests that this is indeed the right choice, although we have not proved it.

As a result, the perturbed system $(V^{(\varepsilon)}(t), G^{(\varepsilon)}(t))$ is ruled by the following ODE:

$$\begin{cases} \dot{V}^{(\varepsilon)}(t) = A \cos(\omega t) - G^{(\varepsilon)}(t)V^{(\varepsilon)}(t), & (a) \\ \varepsilon \dot{G}^{(\varepsilon)}(t) = Q(V^{(\varepsilon)}(t)) - G^{(\varepsilon)}(t). & (b) \end{cases} \quad (67)$$

When development (66) is used up to order 1:

$$\begin{cases} \dot{V}_0(t) + \varepsilon \dot{V}_1(t) = A \cos(\omega t) - G_0 V_0 - \varepsilon(G_0 V_1 + G_1 V_0) + o(\varepsilon), & (a) \\ \varepsilon \dot{G}_0(t) = Q(V_0) - G_0 + \varepsilon(Q'(V_0)V_1 - G_1) + o(\varepsilon), & (b) \end{cases} \quad (68)$$

the zeroth-order terms annihilate each other, and the remaining first-order terms are ruled by

$$\begin{cases} \dot{V}_1(t) = -G_0 V_1 - G_1 V_0, & (a) \\ \dot{G}_0(t) = Q'(V_0)V_1 - G_1. & (b) \end{cases} \quad (69)$$

⁶For $b = 0$, these expansions can be obtained rigorously from an *analytic* version of Picard's fixed point theorem. We have not searched yet the rigorous proof for the expansion near $b = +\infty$.

We have omitted to note the time dependence of all variables on the right-hand side, for the sake of readability.

Fast-slow dynamics. Note that, since parameter ε multiplies the left-hand side of (67-b), it annihilates the possible contribution of $\dot{G}_1(t)$ to the terms of first order in ε . As a consequence, $\dot{G}_1(t)$ is absent from (69-b), meaning that (69-b) is not a differential equation, but a simple equation which directly provides a formula for $G_1(t)$! This property is typical of systems with *fast-slow* dynamics (ε^{-1} being obviously the *fast* time constant), and it allows a considerable simplification of calculations.

Actually, we have already used this *fast-slow* property in Section 4, to define our 1D system $b = +\infty$. Indeed, the annihilation of zeroth-order terms in (68-b) implies that $(V_0(t), G_0(t))$ must verify $G_0(t) = Q(V_0(t))$, which is precisely the heuristic condition we used to derive our 1D system equation.

In other words, the 1D system ‘ $b = +\infty$ ’ defined heuristically in Section 4 can be defined rigorously as the zeroth-order term of the perturbation expansion (66) for $b(\varepsilon) = \varepsilon^{-1}$, provided there is some guarantee of existence for the perturbation expansion.

When system (69) is solved, it yields the following ODE for $V_1(t)$:

$$\dot{V}_1 + L'(V_0)V_1 = \dot{V}_0 R(V_0), \quad (70)$$

where $L(v) = vQ(v)$ and $R(v) = vQ'(v)$. As for $G_1(t)$, it is not an autonomous variable, its formula being imposed by the *fast-slow* dynamics:

$$G_1 = Q'(V_0)V_1 - \dot{G}_0. \quad (71)$$

Interestingly, $V_1(t)$ is ruled by a linear equation (70), so it can be derived from $V_0(t)$ through a close-form equation. Moreover, due to the symmetries of the system, $V_1(t)$ is necessarily $T/2$ -antiperiodic. We can thus apply the same type of integration (over a half-period) as we used to prove equation (40) in Proposition 5. This yields the formula:

$$V_1(t) = \frac{1}{1 + \exp\left(-\int_{t-T/2}^t L'(V_0)\right)} \int_{u=t-T/2}^t \dot{V}_0 R(V_0) \exp\left(-\int_u^t L'(V_0)\right) du, \quad (72)$$

where ‘ V_0 ’ should be read ‘ $V_0(u)$ ’, etc.

We could thus explicitly calculate $V_1(t)$ from our numerical approximation for $V_0(t)$. This allowed us to compare the real solution $(V^{(\varepsilon)}(t), G^{(\varepsilon)}(t))$ and its first order approximation $(V_0(t) + \varepsilon V_1(t), G_0(t) + \varepsilon G_1(t))$. An example is provided in Figure 9. For the given set of parameters, the first and second order approximations provided a relatively good fit up to $\varepsilon \simeq 0.01$ (corresponding to $b \simeq 100$). For higher ε , the approximations (especially second-order) quickly diverged (not shown).

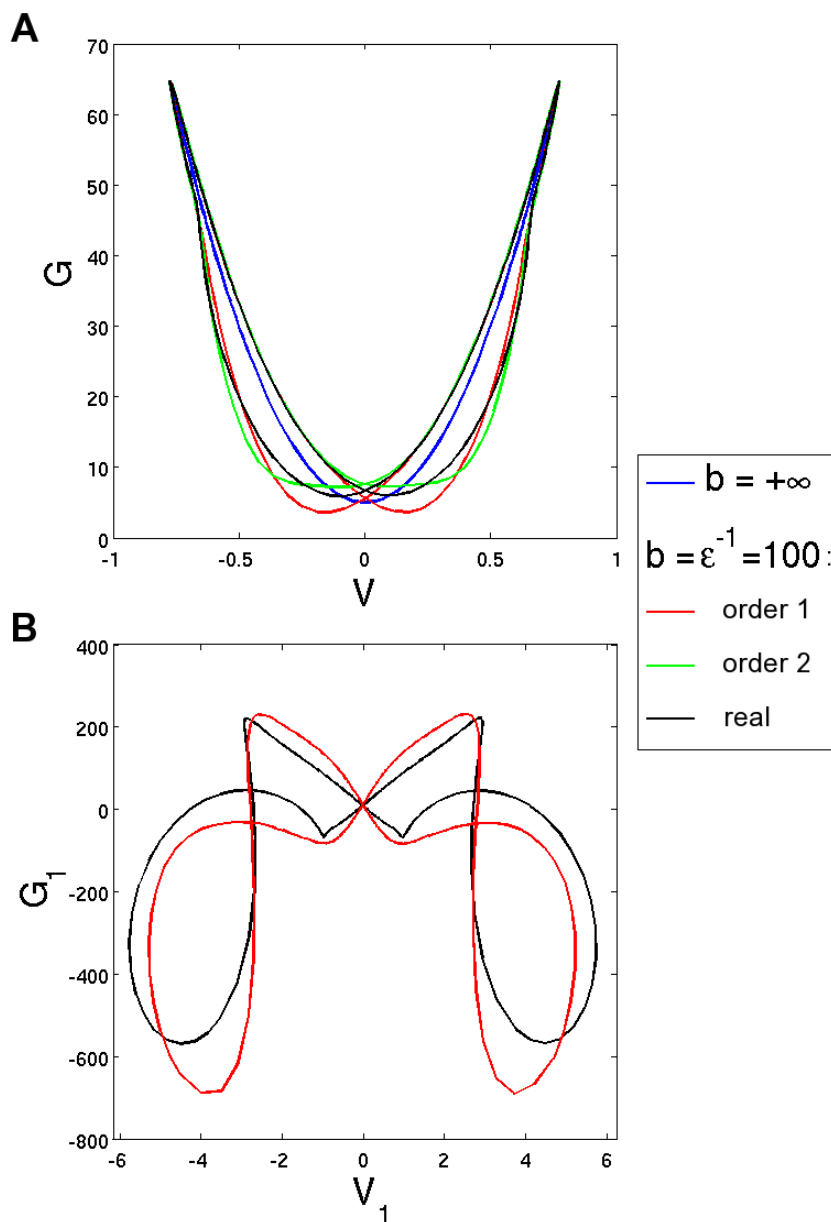


Figure 9: Perturbation analysis near $b = +\infty$. Panel A compares the real solution $(V^{(\varepsilon)}(t), G^{(\varepsilon)}(t))$ to its zeroth, first and second order approximations using perturbation analysis. Panel B compares more specifically the first-order expansion (V_1, G_1) to its approximation by $((V^{(\varepsilon)} - V_0)/\varepsilon, (G^{(\varepsilon)} - G_0)/\varepsilon)$. Perturbation parameter $b = \varepsilon^{-1} = 100$ Hz. Other simulation parameters: $\omega = 2\pi$ Hz, $A = 50$ Hz, $Q(V) = Q_0 + \lambda V^2$ with $Q_0 = 5$ Hz and $\lambda = 100$ Hz.

Higher-order expansions. To conclude, we remark that the type of analysis produced here to derive the first-order expansion (V_1, G_1) applies similarly to all higher order expansions. Indeed, the multiplication by ε in the left-hand side of (67) (*fast-slow* dynamics) insures that, at any order k , function $G_k(t)$ is directly constrained by a formula involving only $V_k(t)$ (not its derivative!), and functions of previous orders. And in turn, $V_k(t)$ is always driven by a linear ODE of the form

$$\dot{V}_k + L'(V_0)V_k = \dots,$$

where the dots denote a combination of functions of previous orders.

This implies that all successive orders can be recursively calculated from the single solution $V_0(t)$ through close-form, linear equations. As a result, the 1D-solution $V_0(t)$ may possibly have a high descriptive power over the whole 2D system.

Because of the relative simplicity of the successive expansions, one could even investigate if some, or all, solutions $(V(t), G(t))$ of the 2D problem can be described by an infinite power series of extensions $(V_k(t), G_k(t))$.

Another question would be to investigate further characterizations of V_{\max} and ϕ_{\max} in the 2D case, and their dependence w.r.t. A , using perturbation analysis. However, even with a good theory for the successive expansions, such results still appear far away.

5.2 Perturbation analysis near $b \rightarrow 0$

Perturbation analysis is also possible near the boundary $b = 0$. The resulting equations for the successive expansions require a different treatment than in the case $b = +\infty$. Generally speaking, the equations are harder to solve near $b = 0$, especially for higher-order expansions.

For this reason, we spend less time on the case $b = 0$. We sketch the main principle to derive the successive expansions (based on what we term a ‘binding condition’), a then provide a result obtained thanks to this ‘binding condition’, in the particular case where $Q(v) = Q_0 + \lambda v^2$ is quadratic.

Note that, although they are harder to manipulate, the expansions near $b = 0$ are also worth studying. Indeed, they can be rigorously justified thanks to an analytic version of Picard’s fixed point theorem (with $b(\varepsilon) = \varepsilon$). Experimentally, the approximations near $b = 0$ also appear more stable than the approximations near $b = +\infty$.

The perturbed system $(V^{(\varepsilon)}(t), G^{(\varepsilon)}(t))$ (for $b(\varepsilon) = \varepsilon$) is ruled by the following ODE:

$$\begin{cases} \dot{V}^{(\varepsilon)}(t) = A \cos(\omega t) - G^{(\varepsilon)}(t)V^{(\varepsilon)}(t), & (a) \\ \dot{G}^{(\varepsilon)}(t) = \varepsilon(Q(V^{(\varepsilon)}(t)) - G^{(\varepsilon)}(t)). & (b) \end{cases} \quad (73)$$

When development (66) is used up to order 1:

$$\begin{cases} \dot{V}_0(t) + \varepsilon \dot{V}_1(t) = A \cos(\omega t) - G_0 V_0 - \varepsilon(G_0 V_1 + G_1 V_0) + o(\varepsilon), & (a) \\ \dot{G}_0(t) + \varepsilon \dot{G}_1(t) = \varepsilon(Q(V_0) - G_0) + o(\varepsilon), & (b) \end{cases} \quad (74)$$

the zeroth-order terms annihilate each other, and the remaining first-order terms are ruled by

$$\begin{cases} \dot{V}_1(t) = -G_0 V_1 - G_1 V_0, & (a) \\ \dot{G}_1(t) = Q(V_0) - G_0. & (b) \end{cases} \quad (75)$$

We have omitted to note the time dependence of all variables on the right-hand side, for the sake of readability. They all depend on time, except for $G_0(t) = G_0$ which is really a constant function (Section 3) !

Binding condition. The particularity of system (75) is that considered as such, it admits an infinity of solutions: Indeed, we have a choice in the integration constant K that will yield $G_1(t)$ from (75-b), and system (75-a) does not restrict our choice for K .

However, if we refer to the *asymptotic* periodic equilibrium of the *real* solution $(V^{(\varepsilon)}(t), G^{(\varepsilon)}(t))$, then (73-b) implies that

$$\widehat{G^{(\varepsilon)}} = Q(\widehat{V^{(\varepsilon)}}), \quad (76)$$

where the hat denotes averaging over one period. We denote this relation the ‘binding condition’ because it allows to bind the choice of constant K to the evolution of $V_1(t)$, and thus to determine $(V_1(t), G_1(t))$ unambiguously. Again, note that the binding condition itself is problematic because it is based on the asymptotic state of the system, which is reached with time constant $\varepsilon^{-1} \rightarrow +\infty$.

When applied to zeroth and first order, the binding condition yields:

$$\widehat{G_0} = \widehat{Q(V_0)}, \quad (77)$$

$$\widehat{G_1} = \widehat{Q'(V_0)V_1}. \quad (78)$$

Note that we have already used this *binding* condition in Section 3, to define our 1D system $b = 0$. Indeed, zeroth-order approximation from (74-b) only yields $\dot{G}_0 = 0$, and we thus needed the binding condition (77) to fully describe our system.

Then, $(V_1(t), G_1(t))$ can be calculated according to the following procedure:

1. Integrate (75-b), yielding a function $G_1(t)$ where the integration constant K is left undetermined.
2. Insert the resulting expression for $G_1(t)$ into (75-a) and solve it formally (it is linear) with constant K still undetermined.
3. Use the binding condition (78) to finally determine K .
4. re-inject the value of K into the calculated expressions for $G_1(t)$ and $V_1(t)$.

We applied this procedure to the particular case where

$$Q(v) = Q_0 + \lambda v^2.$$

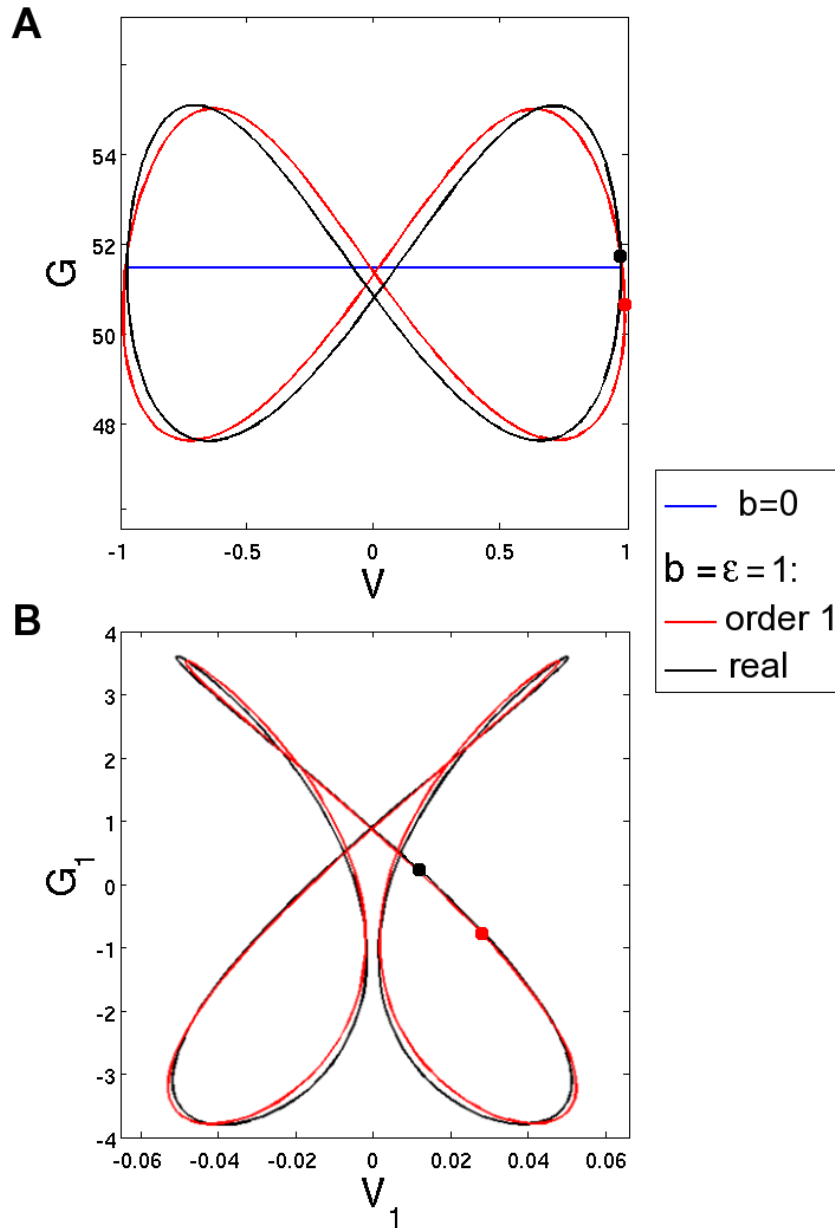


Figure 10: Perturbation analysis near $b = 0$. Panel A compares the real solution $(V^{(\epsilon)}(t), G^{(\epsilon)}(t))$ to its zeroth-, first- and second-order approximations using perturbation analysis. Panel B compares more specifically the first-order expansion (V_1, G_1) to its approximation by $((V^{(\epsilon)} - V_0)/\epsilon, (G^{(\epsilon)} - G_0)/\epsilon)$. The two dots mark the respective positions of the two variables at a given time. Perturbation parameter $b = \epsilon = 1$ Hz. Other simulation parameters: $\omega = 2\pi$ Hz, $A = 50$ Hz, $Q(V) = Q_0 + \lambda V^2$ with $Q_0 = 5$ Hz and $\lambda = 100$ Hz.

First, the zeroth-order binding condition (77) yields

$$(G_0 - Q_0)(G_0^2 + \omega^2) = \frac{\lambda A^2}{2},$$

which can be solved explicitly thanks to Cardan formulas, and from there

$$V_0(t) = \sqrt{\frac{2(G_0 - Q_0)}{\lambda}} \cos(\omega t - \arctan(\omega/G_0)).$$

Second, the procedure described in the previous paragraph yields the following first order expansions:

$$K = -\frac{(G_0 - Q_0)^3}{4G_0(G_0 - Q_0)^2 + \lambda A^2},$$

$$G_1(t) = \frac{G_0 - Q_0}{2\omega} \sin(2(\omega t - \arctan(\omega/G_0))),$$

$$\begin{aligned} V_1(t) &= \frac{(G_0 - Q_0)^2}{2\lambda A} \left(-\frac{1}{\omega} \sin(\omega t - 2 \arctan(\omega/G_0)) + \frac{(G_0 - Q_0)^2}{\lambda A^2 + 2G_0(G_0 - Q_0)} \cos(\omega t - 2 \arctan(\omega/G_0)) \right) \\ &\quad - \frac{\lambda(G_0 - Q_0)}{4\omega \sqrt{(G_0^2 + \omega^2)(G_0^2 + 9\omega^2)}} (\sin(3\omega t - 3 \arctan(\omega/G_0) - \arctan(3\omega/G_0))). \end{aligned}$$

These zeroth and first order expansions are compared to the real trajectory in Figure 10.

Conclusion

As a conclusion, let us remind the practical reason for which we started to lead this study: We wanted to understand better the behavior of the amplitude V_{\max} and phase ϕ_{\max} of $V(t)$, output of our gain control loop, with respect to its input parameters.

The results presented herein prove, through theoretical results and simulations, that the following behavior can be considered true under virtually any sinusoidal stimulation:

1. The system acts as a temporal low-pass filter.
2. The system produces contrast gain control:

$$\partial_A V_{\max} > 0 \quad (\text{growth with contrast}),$$

$$\partial_A \phi_{\max} < 0 \quad (\text{phase advance with contrast}),$$

$$\partial_A \frac{V_{\max}}{A} < 0 \quad (\text{under-linearity with contrast}).$$

From a mathematical point of view, interesting asymptotic behaviors exist for the 2-dimensional system, which live on 1-dimensional spaces and are thus easier to study. Precise mathematical results are available for these 1D asymptotic systems. In the future, perturbation analysis might increase the extent of some results further into the realm of the general 2D system.

References

- [1] W. Lohmiller and J. J. Slotine. On contraction analysis for non-linear systems. *Automatica*, 34(6):683–696, jun 1998.
- [2] Adrien Wohrer. *Model and large-scale simulator of a biological retina with contrast gain control*. PhD thesis, University of Nice Sophia-Antipolis, 2008.
- [3] Adrien Wohrer, Pierre Kornprobst, and Thierry Viéville. Virtual retina: a biological retina model and simulator, with contrast gain control. Research Report 6243, INRIA, jul 2007.



Unité de recherche INRIA Sophia Antipolis
2004, route des Lucioles - BP 93 - 06902 Sophia Antipolis Cedex (France)

Unité de recherche INRIA Futurs : Parc Club Orsay Université - ZAC des Vignes
4, rue Jacques Monod - 91893 ORSAY Cedex (France)

Unité de recherche INRIA Lorraine : LORIA, Technopôle de Nancy-Brabois - Campus scientifique
615, rue du Jardin Botanique - BP 101 - 54602 Villers-lès-Nancy Cedex (France)

Unité de recherche INRIA Rennes : IRISA, Campus universitaire de Beaulieu - 35042 Rennes Cedex (France)

Unité de recherche INRIA Rhône-Alpes : 655, avenue de l'Europe - 38334 Montbonnot Saint-Ismier (France)

Unité de recherche INRIA Rocquencourt : Domaine de Voluceau - Rocquencourt - BP 105 - 78153 Le Chesnay Cedex (France)
